



HAL
open science

Profiling target genes of FGF18 in the postnatal mouse lung: possible relevance for alveolar development.

Marie-Laure Franco-Montoya, Olivier Boucherat, Christelle Thibault, Bernadette Chailley-Heu, Roberto Incitti, Christophe Delacourt, Jacques R. Bourbon

► **To cite this version:**

Marie-Laure Franco-Montoya, Olivier Boucherat, Christelle Thibault, Bernadette Chailley-Heu, Roberto Incitti, et al.. Profiling target genes of FGF18 in the postnatal mouse lung: possible relevance for alveolar development.. *Physiological Genomics*, 2011, 43 (21), pp.1226-40. 10.1152/physiolgenomics.00034.2011 . inserm-00647306

HAL Id: inserm-00647306

<https://inserm.hal.science/inserm-00647306>

Submitted on 30 Aug 2012

HAL is a multi-disciplinary open access archive for the deposit and dissemination of scientific research documents, whether they are published or not. The documents may come from teaching and research institutions in France or abroad, or from public or private research centers.

L'archive ouverte pluridisciplinaire **HAL**, est destinée au dépôt et à la diffusion de documents scientifiques de niveau recherche, publiés ou non, émanant des établissements d'enseignement et de recherche français ou étrangers, des laboratoires publics ou privés.

1 **Profiling target genes of FGF18 in the postnatal mouse lung:**
2 **possible relevance for alveolar development**

3

4 **Marie-Laure Franco-Montoya,^{1,2,3} Olivier Boucherat,⁴ Christelle Thibault,⁵ Bernadette**
5 **Chailley-Heu^{1,2}, Roberto Incitti,^{1,2} Christophe Delacourt,^{1,2,3} and Jacques R. Bourbon^{1,2,3}**

6

7 *¹INSERM, Unité 955-IMRB, Équipe 04, Créteil, France ; ²Faculté de Médecine, Université Paris-Est Créteil Val*
8 *de Marne, France ; ³PremUP, Paris, France ; ⁴Centre de Recherche en Cancérologie de L'Hôtel-Dieu de*
9 *Québec, Université Laval, Québec, Canada; ⁵Institut de Génétique et de Biologie Moléculaire et Cellulaire*
10 *(IGBMC), Illkirch, France*

11

12

13 Address for correspondence: M-L Franco-Montoya, INSERM U955-IMRB, Faculté de Médecine, 8

14 rue du Général Sarrail, 94010 Créteil, France (e-mail : marie-laure.franco-montoya@inserm.fr).

15 Tel: +33 – 1 49 81 35 16

16 Fax: +33 – 1 48 98 17 77

17

18

19

20 **Running head:** FGF18 target genes in postnatal lung

21

22 **ABSTRACT**

Better understanding alveolarization mechanisms could help improve prevention and treatment of diseases characterized by reduced alveolar number. Although signaling through fibroblast growth factor (FGF) receptors is essential for alveolarization, involved ligands are unidentified. FGF18, the expression of which peaks coincidentally with alveolar septation, is likely to be involved. Herein, a mouse model with inducible, lung-targeted FGF18-transgene was used to advance the onset of FGF18 expression peak, and genome-wide expression changes were determined by comparison with littermate controls. Quantitative RT-PCR was used to confirm expression changes of selected up and down regulated genes, and to determine their expression profiles in the course of lung postnatal development. This allowed identifying so far unknown target genes of the factor, among which a number are known to be involved in alveolarization. The major target was adrenomedullin, a promoter of lung angiogenesis and alveolar development, whose transcript was increased 6.9-fold. Other genes involved in angiogenesis presented marked expression increases, including *Wnt2* and *cullin2*. Although it appeared to favor cell migration notably through enhanced expression of *Snai1/2*, FGF18 also induced various changes consistent with prevention of epithelial-mesenchymal transition. Together with anti-fibrotic effects driven by induction of E prostanoid receptor 2 and repression of numerous myofibroblast markers, this could prevent alveolar septation-driving mechanisms from becoming excessive and deleterious. Last, FGF18 up or down regulated genes of ECM components and epithelial-cell markers previously shown to be up or down regulated during alveolarization. These findings therefore argue for an involvement of FGF18 in the control of various developmental events during the alveolar stage.

23

24

25 **Key words:** transgenic mice, alveolarization, angiogenesis, fibrosis, epithelial-mesenchymal
26 transition.

27

28 INTRODUCTION

29 Lung alveolarization, the formation process of definitive alveoli, is a complex developmental event
30 that extends from the last gestational weeks to the 2 first postnatal years. In rats and mice that are
31 classical model animals for studying its underlying mechanisms, it is entirely postnatal; subdivision of
32 alveolar sacs by secondary septation takes place between days 4 and 14 (although recent investigations
33 have indicated that new alveoli can be generated later from mature septa), and septal maturation with
34 fusion of double capillary layer into a single layer is terminated on day 20. Alveolarization involves a
35 variety of regulatory factors, but its control is only partially understood (5) . Deciphering these
36 mechanisms is of particular importance because they are profoundly disturbed in chronic lung disease
37 of the premature neonate also known as “new” bronchopulmonary dysplasia (BPD) (19) or in lung
38 hypoplasia consecutive to congenital diaphragmatic hernia (CDH) (3) . Furthermore, maintenance of
39 alveolar structure necessitates the persistence of at least some of these control pathways in the adult
40 lung, which appears to be disordered in emphysema (6).

41 Alveolarization is abolished in mice simultaneously devoid of fibroblast growth factor (FGF)
42 receptors (FGFR) 3 and 4 (49). Despite normal elastic fiber gene expression in isolated lung interstitial
43 cells, excessive elastin deposition occurs in this model with loss of typical spatial restriction, and
44 epithelial cells contribute to the observed abnormalities (42). Thus far however, the identity of
45 involved FGF(s) has remained elusive. The assumption that FGF18 is involved is based on the facts
46 that (i) this mediator, similar to the most homologous other FGF-family members FGF8 and FGF17,
47 binds FGFR4 and the IIIc-form of FGFR3 with high affinity (12, 39), and (ii) a strong rise of FGF18
48 expression occurs when secondary septation starts in 3 species, namely the rat (7), the mouse (8, 30)
49 and man (3). Most strikingly, secondary septation coincides precisely with the peak of lung FGF18
50 expression that falls abruptly after its ending in the rat and the mouse (7, 8, 30). Indeed, FGF18 level
51 could not be studied until completion of alveolar development in man because this occurs during the
52 second postnatal year.

53 Although it is expressed at a lower rate earlier, there are evidences for FGF18 involvement in
54 previous lung developmental stages already. Conditional expression of FGF18 in the lung of
55 transgenic mouse fetuses from embryonic day 6 to term thus caused distal airways to adopt structural

56 features of proximal airways with abnormal cartilage deposition, suggesting a role in the control of
57 proximal differentiation program during pseudoglandular/canalicular stages (51). FGF18 was
58 accordingly reported to control chondrogenesis in upper airways (11). These findings, however, do not
59 enlighten the functional significance of the marked postnatal peak of FGF18 expression, when the
60 tract of cartilage-containing conducting airways is complete. Another investigation evidenced reduced
61 air space, thicker interstitial mesenchymal compartments, and presence of embedded capillaries in the
62 prenatal lung consequently to *Fgf18* gene targeting in mice, which indicates involvement at saccular
63 stage also (45). Consistently, FGF18 expression was found to be enhanced in the stimulation of fetal
64 rat lung growth induced by tracheal ligation (34). Unfortunately, FGF18 gene targeting cannot be used
65 to investigate FGF18 role during alveolar stage because *Fgf18*^{-/-} pups do not survive beyond birth.

66 Although FGF18 implication in alveolarization has therefore not yet received demonstration, it is
67 nevertheless further supported indirectly by several observations. Thus, FGF18 stimulated *ex vivo*
68 proliferation of perinatal rat lung fibroblasts and enhanced their expression of elastic fiber components
69 (7), two events that occur during alveolar septation. Last, although FGF18 is unexplored in BPD,
70 decreased FGF18 expression was found to be associated with impaired alveolarization in 2 instances,
71 (i) a rat model of BPD (28) and (ii) human lung hypoplasia consecutive to CDH (3).

72 To document the molecular effects of FGF18 and try to explore the physiological significance of its
73 sharp postnatal expression peak, the Tet-On system-based mouse model of conditional FGF18
74 expression in the lung designed by Whitsett et al. (51) was used here to provoke a rise of FGF18 in the
75 perinatal period, hence inducing precociously an increase of expression similar to the one occurring
76 after birth during secondary alveolar septation. Pups were collected before the onset of septation, i.e.
77 before the rise of endogenous FGF18. This timing was chosen because we assumed that inducing the
78 expression of the transgene later, during the stage of secondary septation, might have added little to
79 the effects of endogenous FGF18-gene expression. In view of the considerable rise of the latter during
80 this stage, responses are likely to be high, and even possibly maximal. Gene profiling study was then
81 performed on genome-wide expression microarrays to identify genes up or down regulated by induced
82 FGF18 expression. Double transgenic mouse pups bearing both the inducible FGF18 transgene and
83 the inducer construct were compared to controls bearing only the silent FGF18 transgene. Some of the

84 affected genes were selected on the basis of both their known functions and the extent of FGF18
85 effects to confirm changes by quantitative RT-PCR and to determine their expression profile during
86 postnatal development. We thus identified as FGF18 targets a variety of genes the involvement of
87 which in alveolarization is either demonstrated or likely, which argues for specific FGF18 functions in
88 postnatal lung development.

89

90 **MATERIAL AND METHODS**

91 **Wild type mice, transgenic mice and treatments**

92 Wild type FVB/N mice were purchased from Charles River Laboratories (Saint Germain sur
93 l'Arbresle, France). The transgenic mouse model has been described in detail previously (45). In brief,
94 mice bearing the inducible construct (teto)₇-CMV-FGF18 transgene were bred to SP-C-rtTA mice in
95 which the expression of the rtTA activator construct is targeted on alveolar epithelial type II cells by
96 the promoter of surfactant protein C. Mice bearing the transgenic constructs were bred in an FVB/N
97 background from two male founders obtained from the Cincinnati Children's Research Foundation.
98 Animal experiments were performed under license from the Animal Health and Protection Service of
99 the French Ministry of Agriculture. Because FGF18 expression in mouse lung increases postnatally to
100 peak on days 7 to 10 (8, 30), the inducer doxycycline was given from prenatal day 2 (E18) to postnatal
101 day 2 (P2) in order to induce earlier an expression peak similar to the one occurring during alveolar
102 septation. Pup lungs were collected aseptically on P3 under pentobarbital anesthesia and kept frozen at
103 -80°C until use or fixed at constant pressure for histological analysis. Experimental protocol is
104 summarized in Fig.1.

105

106 Lung morphology and morphometry

107 Methods used in this study have been described in detail previously (28). Briefly, lung fixation was
108 performed by tracheal infusion of neutral buffered paraformaldehyde at constant 20cm H₂O pressure,
109 and fixed lung volume was measured by fluid displacement. After routine processing and paraffin
110 embedding, 4- μ m-thick mediofrontal sections through both lungs were stained with picro-indigo-
111 carmine for morphological pictures or with hematoxylin-phloxine-saffron for morphometry. Alveolar

112 airspace, airways, blood vessels larger than 20 μm in diameter, interstitial tissue volume densities and
113 the alveolar surface density were determined using the point counting and mean linear intercept
114 methods (48). Light microscope fields were quantified at an overall magnification of x440 on 20 fields
115 per animal (10 per lung) with a systematic sampling method from a random starting point. All
116 morphometric analyses were performed by a single observer (BCH) who was unaware of group
117 assignment.

118

119 **Genotyping and assessment of FGF18-transgene expression**

120 Genotyping was performed on DNA extracted from mouse-tails by use of the ChargesSwitch® gDNA
121 kit Mini Tissue kit from Invitrogen (Cergy-Pontoise, France) using the following primers for PCR in a
122 Hybaid thermocycler: for SP-C-rtTA, 5'-GACACATATAAGACCTGGTC-3' (forward) and (5'-
123 AAAATCTTGCCAGRCTTCCCC-3' (reverse); for (teto)₇-FGF18, 5'-GCCATCCACGCTCTTTG-3'
124 (forward primer located in the CMV minimal promoter) and 5'-
125 CAGGACTTGAATGTGCTTCCCACTG-3' (reverse primer located in the FGF18 cDNA). The two
126 last primers were also used in doxycycline-treated pups to assess specifically the FGF18-transgene
127 expression response by semi-quantitative RT-PCR on total RNAs extracted from lung tissue.
128 Quantitative RT-PCR for total FGF18 transcript was performed as described below (primers in table
129 1).

130

131 **Generation of cRNA “target” and chip hybridization**

132 Total RNA was extracted from lung tissue using the guanidinium isothiocyanate method (TRIzol
133 reagent, Invitrogen, Cergy-Pontoise, France), followed by purification using Rneasy columns (Qiagen,
134 Courtaboeuf, France). Four pairs of control ((teto)₇-CMV-FGF18) and double-transgenic (SP-C-rtTA ,
135 (teto)₇-CMV-FGF18) pups, each pair being issued from a different litter (i.e. 4 different litters and 4
136 biological replicates for each condition) were selected on the basis of FGF18 transgene induction.
137 Integrity and purity of RNA were checked by spectrophotometry and capillary electrophoresis, using
138 the Bioanalyser 2100 and RNA 6000 LabChip kit from Agilent Technologies (Palo Alto, CA). cDNAs
139 and biotin-labeled-cRNAs were successively synthesized using Superscript Choice system

140 (Invitrogen) and Affymetrix IVT labeling kit (Affymetrix, Santa Clara, CA, USA), respectively. After
141 purification, 10 µg of fragmented cRNA were hybridized to the Affymetrix GeneChip® Mouse
142 Genome 430 2.0 Array (>39,000 transcripts). Each of the 4 control samples and of the 4 double-
143 transgenic samples was hybridized individually on one chip (no technical replicates). Chips were
144 automatically washed and stained with streptavidine-phycoerythrin. Arrays were scanned at 570 nm
145 with a resolution of 1.56 µm/pixel using Affymetrix Gene Chip Scanner 3000. Expression values were
146 generated using Microarray Suite v5.0 (MAS5, Affymetrix). Each sample and hybridization
147 experiment underwent a quality control evaluation (table 2).

148

149 **Microarray data analysis**

150 Gene expression values were extracted from cell-probe values using the affy package (16) of the R
151 software (15). Rma2 implementation of Robust Multiarray Averaging (17), qspline (55), pmonly and
152 liwong (25) were used as methods of background correction, normalization, pm-correction and
153 summarization, respectively. In order to assess replicability, the pair-wise correlations were computed
154 between the 8 arrays. The lowest value (0.976266) indicated excellent overall replicability.
155 Concerning intra-condition replicability, lowest values were 0.9921674 for controls and 0.979491 for
156 double-transgenic pups. For gene selection, a one-tailed *t*-test for paired values was computed for both
157 over and under-expressions. Paired *t*-test was used because each of the 4 double-transgenic pups was
158 compared to its corresponding littermate control that had experienced same environment during the
159 experiment. Because directional changes were searched for, i.e. gene expressions presenting univocal
160 increases or decreases in all the 4 double-transgenic samples, a one-tailed *t*-test was used. Features
161 were then ranked with respect to their *P*-value, and the list of features in the best 1% was determined.
162 We computed the mean of the logratios, ranked the features and selected the top 0.5 for each direction
163 of differential expression. The intersection of those 2 lists was selected for further analysis.

164

165 **Reverse transcription (RT) and real-time quantitative polymerase chain reaction (qPCR)**

166 RNAs extracted as described above were reverse-transcribed into cDNAs using 2 µg of total RNA,
167 Superscript II reverse transcriptase, and random hexamer primers (Invitrogen) according to the

168 supplier's protocol. Real-time PCR was performed on ABI Prism 7000 device (Applied Biosystems,
169 Courtaboeuf, France) using initial denaturation (10 min at 95°C), then two-step amplification program
170 (15 s at 95°C followed by 1 min at 60°C) repeated 40 times. Melt curve analysis was used to check
171 that a single specific amplified product was generated. Reaction mixtures consisted of 25 ng cDNA,
172 SYBR Green 2X PCR Master Mix (Applied Biosystems), and forward and reverse primers for the
173 various examined transcripts (displayed in table 1) in a reaction volume of 25 μ l. Primers were
174 designed using Primer Express software (Applied Biosystems). Real-time quantification was
175 monitored by measuring the increase in fluorescence caused by the binding of SYBR Green dye to
176 double-stranded DNA at the end of each amplification cycle. Relative expression was determined by
177 using the $\Delta\Delta$ Ct (threshold cycle) method of normalized samples (Δ Ct) in relation to the expression of
178 a calibrator sample used to normalize data from one plate to another, according to the manufacturer's
179 protocol. Each PCR run included a no-template control and a sample without reverse transcriptase. All
180 measurements were performed in triplicates. Both 18S rRNA and the housekeeping gene *Hprt1*
181 mRNA were used as references and provided similar values (see below, Results section). For in vivo
182 effects of FGF18-transgene induction, individual data were expressed as a percentage of the mean
183 control value (single-transgenic pups) in each litter. For developmental expression profiles (lungs of
184 wild type mice), data were expressed as percentage of P0 (neonates) level. Control and double-
185 transgenic comparisons of gene-expression directional changes were made by one-tailed *t* test. For
186 developmental expression profiles, considering the small sample size (4 individuals from 2 different
187 litters per stage), non-parametric tests were used: multiple stage comparisons were made by Kruskal-
188 Wallis analysis, followed by two-stage comparisons by Mann and Whitney U test.

189

190

191 **RESULTS**

192 **FGF18-transgene expression and lung morphology/morphometry in doxycycline-treated mouse**
193 **pups**

194 As evaluated on P3, induction of FGF18 transgene in the lung was observed in all litters, although its
195 rate varied widely among individuals and litters. In the 4 double-transgenic individuals selected for
196 chip hybridization, FGF18 transgene amplification was manifest as estimated by semi-quantitative
197 RT-PCR run with specific primers (Fig. 2). In those samples, quantification of total FGF18 expression
198 by microarray analysis indicated 11.7-fold average increase (range: 1.5- to 20-fold), and that by RT-
199 qPCR 6.35-fold average increase (range: 1.8- to 22-fold). In the 11 double-transgenic pups from 5
200 different litters used to confirm by RT-qPCR the changes evidenced by microarray data, it was
201 similarly increased over 6-fold as compared to 10 single-transgenic littermates ($2^{\Delta\Delta Ct}$: 13.37 ± 2.96 vs
202 2.14 ± 0.16 , respectively, and $641.9 \pm 143.1\%$ of controls vs $100.0 \pm 6.3\%$, $P < 0.001$). Although the
203 level might have varied along treatment, this is indicative of the extent of transgene induction.
204 Morphology of lung parenchyma appeared unaffected in double transgenic pups as compared to either
205 wild-type or single-transgenic pups (Fig. 3). Morphometric analysis performed on pups that had
206 undergone the same doxycycline-treatment protocol as those used for gene-expression analysis
207 indicated no significant change in double-transgenic pups for lung volume, mean linear intercept, or
208 alveolar surface area, either on P4 when secondary septation starts, or on P8 or P16 when it is more
209 advanced and terminated, respectively (table 3).

210

211 **Array data analysis**

212 Primary microarray data are available at the Gene Expression Omnibus Database
213 (www.ncbi.nih.gov/geo/ GEO accession number: GSE22283). Statistical analysis retrieved 487 genes
214 and EST significantly up-regulated, and 1235 genes and EST significantly down-regulated by FGF18
215 induction. Only characterized genes with defined function(s) were considered further. Fold-change of
216 the 77 up-regulated genes ranged from 1.12-fold to 4-fold their respective basal expression levels in
217 single-transgenic controls. Maximum expression decrease of down regulated genes was about 70%. In
218 order to avoid exceedingly large tables and discussion about limited expression changes only genes

219 with expression increased or decreased at least 25% are displayed in tables 4 and 5, respectively (i.e.
220 32 up-regulated genes including five genes of particular interest increased 22.4 to 24.2%, and 104
221 down-regulated genes).

222 Data from RT-qPCR determinations used to confirm expression changes of selected genes and to
223 determine their developmental expression profiles were referred to both 18S rRNA and Hprt1 mRNA.
224 Although absolute values provided by both references were slightly different, they indicated the same
225 proportional changes (Table 6). The use of either reference therefore did not affect conclusions.
226 Because 18S rRNA level displayed constant proportionality with the amount of extracted RNAs and
227 more stable $2^{-\Delta\Delta ct}$ (i.e. more constant level) than Hprt1 mRNA across the developmental period under
228 study, data presented below are those using 18S rRNA as reference.

229

230 **Genes up regulated by FGF18 induction**

231 To facilitate comparisons, the developmental profile of endogenous FGF18 is presented along with
232 those of genes up regulated by FGF18-transgene induction (Fig. 4, bottom). FGF18 transcript was
233 enhanced on P4 and further on P7 as compared with P0 level, then dropped on P14 and further on P28,
234 and reached very low level in adult lung. Following transgene induction, the gene with most strongly
235 increased expression (4-fold) was that of the vasoactive peptide adrenomedullin (Adm). RT-qPCR
236 analysis on a larger number of pups indicated even stronger stimulation (almost 6.9-fold, table 7).
237 Adm was followed by CD36 antigen (also known as fatty acid translocase), and hydroxysteroid 11 β
238 dehydrogenase 1 (Hsd11b1), which was confirmed by RT-qPCR although changes were found to be
239 slightly (CD36) or largely (Hsd11b1) higher than those detected by microarrays (table 7). The
240 postnatal expression profiles of these 3 genes in normal lung shared a 2.5- to 5-fold decrease between
241 days P0 and P4 (Fig. 4), an event that appeared to have been prevented by FGF18 induction in
242 transgenic pups. This was followed by re-increase from P4 but with different patterns. Adm transcript
243 rose sharply from P4, peaked from P7 to P14, then fell to retrieve low level on P20 onwards (Fig. 4),
244 displaying therefore a profile resembling that of endogenous FGF18 expression, except for the P4
245 decrease. CD36 expression also re-increased rapidly from P4 whereas that of Hsd11b1 re-increased

246 more gradually, but contrary to Adm, both maintained high level until day 28 and returned to low level
247 in adult lung only (Fig. 4). CD36 expression level varied widely among individuals.

248 In addition to fibulin 1 expression already known to be enhanced by FGF18 (7), the expression of
249 various extracellular matrix (ECM) components was increased. These include bone sialoprotein (or
250 integrin binding sialoprotein, Ibsp), chondroitin sulfate proteoglycan 2 (table 4), and chondromodulin-
251 1b (not included in table 4). RT-qPCR confirmed bone sialoprotein and fibulin 1 changes, the steady-
252 state level of their transcripts being increased 2.8 times and 1.69 times, respectively (table 6). Their
253 developmental profiles presented high level during the period of secondary septation and a drop on
254 day 14 (Fig. 4), consistent with control by endogenous FGF18.

255 FGF18 induction up-regulated the expression of a variety of genes involved in antioxidant
256 metabolism, including glutathione-S-transferase mu5 (Gstm5), ceruloplasmin, leucine-rich α 2-
257 glycoprotein-1 (Lrg1) cytochrome P450 (Cyp) 2e1, cysteine dioxygenase 1, adrenodoxin (table 4),
258 serine hydroxymethyl transferase, carbonyl reductase 1, and SH3-binding domain glutamic acid-rich
259 protein like (Sh3bgr1) (not included in table 4). Again, expression changes determined by RT-qPCR
260 for the mostly affected genes Gstm5 and ceruloplasmin were larger than those from microarrays,
261 reaching 3.2-fold and 2.6-fold, respectively (table 7). Gstm5 developmental expression profile
262 displayed increase from P4 to P7, fall on day 14, and further decrease to very low level in adulthood,
263 consistent with control by endogenous FGF18 (Fig. 4). By contrast, that of ceruloplasmin displayed
264 postnatal decrease, no significant change from P4 to P10, moderate decrease on P14, increase on P28,
265 and maintenance of sizeable level in adult lung, which argues for multifactorial control involving
266 factors other than FGF18.

267 FGF18 induction also more or less enhanced (+50% to +16%) the expression of genes the protein
268 products of which are known to stimulate or are likely to be involved in cell migration, including
269 wingless-related MMTV integration site 2 (Wnt2), snail homologs 1 and 2 (Snai1, Snai2), sushi-repeat
270 protein, mixed-lineage kinase-like mitogen-activated triple kinase alpha (MLTK α), and neural
271 precursor cell-expressed developmentally down-regulated gene 9 (Nedd9). Importantly, it
272 simultaneously stimulated (+100% to +16.5%) the expression of genes the products of which have
273 opposite and antifibrotic effects, including (in addition to CD36 antigen already mentioned) Th2-

274 specific cytokine FISP/IL24, Borg4/binder of Rho GTPase 4, prostanoid E receptor EP2 subtype
275 (Ptger2) (table 4), and the tumor suppressor Lim domains-containing protein 1 (Limd1, not included in
276 table 4). RT-qPCR analysis run for Wnt2, Snai1, Snai2, and Ptger2 confirmed enhancement with
277 larger changes than those detected by microarray analysis (table 7), particularly marked for Wnt2 and
278 Snai2 (2.4-fold each). Developmental expression profiles of these 4 genes were very similar, with high
279 level during alveolar septation, maximum on P7-10, abrupt drop on P14, and low level during
280 alveolar-wall maturation and in adult lung (Fig. 4), consistent with regulation by FGF18.

281 Last, in keeping with its effects on lung-fibroblast proliferation (7), FGF18 enhanced the
282 expression of a variety of genes involved in cell growth and ribosome synthesis, including G0G1
283 switch gene 2, brix domain containing 1 (Bxdc1), NIMA-related expressed kinase 8 (Nek8) (table 4),
284 and more slightly (not included in table 4), mitogen activated protein kinase kinase 1 (Map2k1),
285 mitogen activated protein kinase kinase kinase 8 (Map3k8), cyclin D2, ribosomal proteins S2 and S13,
286 mitochondrial-ribosomal protein S18B, and WD repeat domain 12 (Wdr12).

287

288 **Genes down regulated by FGF18 induction**

289 Six genes presenting over 50% decreased expression (table 5) included the adipocyte markers (also
290 expressed in alveolar type II cells) C1q and tumor necrosis factor related protein 3 (C1qtnf3 or
291 CTRP3, also known as cartducin, cartonectin, or collagenous repeat-containing sequence of 26kDa
292 protein [CORS 26]), stearoyl-Coenzyme A desaturase 1 (Scd1), and Ca⁽²⁺⁾-sensitive chloride channel
293 2, the alveolar type II cell marker ATP-binding cassette transporter 3 (ABCA3), the ECM component
294 osteoglycin (Ogn), and the ECM-degrading enzyme, fibroblast activation protein (Fap) also designated
295 Seprase. Other ECM and connective tissue components, including proteoglycan 4, chondrolectin,
296 asporin, matrilins 1 and 2, thrombospondin 4 and chondroadherin, and another ECM-degrading
297 enzyme, Adamts 5, had notably reduced expression (-47% to -30%, table 5). The transcript of the
298 transcription factor high mobility group box protein / SRY-box containing gene (Sox2), another gene
299 with epithelium-restricted expression, was reduced by 40%. RT-qPCR analysis confirmed the decrease
300 for C1qtnf3, Scd1, ABCA3 (-49%, -69%, -48%, respectively), but not for Sox 2, Ogn and Fap (table
301 8). As regards Sox 2, Ogn and Fap, although RT-qPCR confirmed lower levels in those samples used

302 for microarray hybridization, the variability between and inside litters was so wide for single- as well
303 as for double-transgenic pups that no significant change was observed on the average in the 11 double-
304 transgenic pups compared to their 10 control littermates. Moreover, there was no correlation between
305 individual values and the extent of FGF18 changes in double-transgenic pups, suggesting the
306 fortuitous character of variations. Developmental expression profiles were established for *C1qtnf3*,
307 *Scd1* and *ABCA3* (Fig. 5). *C1qtnf3* transcript rose from P0 to P4, which was unlikely to be related to
308 endogenous FGF18, decreased then gradually until P14, which could relate to FGF18 peak, and
309 decreased further until adulthood. *Scd1* transcript increased modestly from P4 to P14, then strongly
310 until P28 to decline in adult lung. *ABCA3* transcript declined half on P4, rose about twice on days 7-
311 10, which could indeed not be due to endogenous FGF18, then decreased about twice on P14 and
312 remained stable thereafter.

313 Two genes whose protein products are related to retinoic acid (RA) metabolism, cellular RA
314 binding protein 1 (*Crabp1*), aldehyde dehydrogenase family 1, subfamily A1 (*Aldh1a1*) displayed
315 reduced expression in microarray findings (-45% and -40%, respectively). This was confirmed by RT-
316 qPCR for *Crabp1* (-59%) but not for *Aldh1a1* for the same reasons as above (table 8). However,
317 *Crabp1* developmental profile presented huge increase from P4 to P14 and decreased then
318 progressively to extremely low level in adult lung (Fig. 5). This profile is not consistent with a
319 negative control by endogenous FGF18 since both transcripts evolve in parallel during development.

320 FGF18 induction reduced to variable extent the expression of various genes related with cell
321 migration and invasion, including doublecortin (*Dcx*, -48%), plasminogen activator inhibitor type II
322 (*PAI2/Serpinb2*, -39%), cytoplasmic polyadenylation element binding protein (*Cpeb*, -30%), and
323 semaphorin 5A (-29%) (table 5), and more modestly *PAI1/Serpine 1* (-23%, not included in table5).
324 RT-qPCR analysis of *Dcx* confirmed decrease (table 7). As for *Crabp1*, *Dcx* developmental expression
325 profile looked similar to that of FGF18 with peak from P7 to P10 and fall on P14 (Fig. 5), which
326 indicates that endogenous FGF18 does not exert negative control.

327 In addition to *ABCA3*, FGF18 induction reduced the expression of a variety of alveolar and/or
328 bronchiolar (*Clara*) epithelial cell markers, including cytochrome oxidases *Cyp1b1* (confirmed by RT-
329 qPCR, table 7), *Cyp2f2* and *Cyp2b10*, aquaporins 3 and 4, uteroglobin-related protein

330 1A/secretoglobin (Scgb3a2), aldehyde oxydase 3, and claudin 8. Expressions of other genes related
331 with oxidant/detoxification/xenobiotic metabolism, namely Cyp2b20, Cyp4b20, Cyp2f2, cytochrome
332 oxydase subunits VIIa and VIIIb, vanin1 (table 5), and Cyp2b20 (-21%, not included in table 5), were
333 also diminished. The developmental expression profile of Cyp1b1 was consistent with down
334 regulation by endogenous FGF18: initially elevated at birth, it decreased abruptly to minimum level
335 maintained from d7 to d20, re-increased slightly on d28, and decreased again in adult lung (Fig. 5).

336 Last, FGF18 induction decreased the expression of a variety of contractile cell markers, including
337 troponins C, I and T3, myomesin 1, chondrolectin, actinin alpha 2, mouse alpha cardiac myosin heavy
338 chain, calponin 1, myomesin 2, actins gamma 2 and alpha 1, dystrophin, caveolin 3, and calsequestrin
339 2 (-45% to -25%, table 5). Interestingly, expression of the specific myofibroblast markers calponin 1
340 (table 5) and α -smooth-muscle actin (more slightly diminished, not shown in table 5) was also
341 reduced.

342

343 **DISCUSSION**

344 Using a mouse transgenic model, we found that advancing the peak of pulmonary FGF18 expression
345 affected the expression level of numerous genes in a variety of pathways. Despite apparent
346 complexity, most of these effects can be filed into 3 main groups that deal with (i) angiogenesis, (ii)
347 cell migration, and (iii) expression of ECM components. Although alveolarization was not advanced
348 by FGF18 induction, these effects are suggestive of FGF18 involvement in alveolarization
349 mechanisms.

350

351 **Putative FGF18 target cells in the lung considering FGF18 receptor expression.**

352 FGF18 binds with high affinity the IIIc splice variant of FGFR3 and the unique form of FGFR4, and
353 more modestly the IIIc splice variant of FGFR2, but presents no affinity for IIIb isoforms (12, 39).
354 Considering FGFR expression pattern, all cell types of lung parenchyma are potential targets of
355 FGF18 through one or two receptors. Thus, if FGFR2 IIIc variants are expressed exclusively in
356 mesenchyme-derived tissues, both lung mesenchymal and alveolar epithelial cells express FGFR3 and
357 FGFR4 (41), although it is unknown whether they express differentially FGFR3IIIb and IIIc.

358 Pulmonary endothelial cells and vascular smooth muscle cells are likely to express FGFR2IIIc and
359 FGFR3IIIc, since these have been characterized in human umbilical vascular endothelial cells
360 (HUVEC) and aortic smooth muscle cells (2). Indeed, direct although different biological effects of
361 FGF18 have been demonstrated on cultured cells of the different types. Specifically, FGF18 enhanced
362 lung fibroblast proliferation and let unchanged epithelial-cell proliferation (7), whereas it induced
363 BMP4 expression in tracheal epithelial cells (14). HUVEC displayed chemotaxis toward FGF18, but
364 failed to proliferate in response to the factor (1). Studying changes in gene expression level in whole
365 lung therefore allows one to detect changes occurring in any of potential target cells. However, this
366 prevents from identifying any compartmentalization influence, except for genes known to present
367 expression restricted to one cell type. The present study should therefore be completed by future
368 investigations aiming at spatial determination of FGF18 effects.

369

370 **Limitations of the study.**

371 One could raise an objection that lack of morphological changes after precocious induction of FGF18
372 expression argues against the involvement of the factor in alveolarization mechanisms. However,
373 considering the complexity of alveolarization and the multiplicity of involved control factors (5) it is
374 not surprising that the induction of a single factor, even if actually involved, was insufficient alone to
375 induce precociously the whole process. More questionable are apparently paradoxical effects of
376 transgenic FGF18 such as markedly increased CD36 and Hsd11b1 expressions. Although endogenous
377 FGF18 might contribute to their expression re-increase from P4, their profiles, contrary for instance to
378 that of Adm, do not coincide with that of FGF18. Hsd11b1 expression remains at low relative level
379 during septation when FGF18 peaks. CD36 expression remains elevated and that of Hsd11b1 continues
380 increasing when FGF18 expression falls to maintain maximal level until P28, i.e. 14 days after FGF18
381 fall down. This appears inconsistent with control by FGF18 only, and presumably results from
382 complex changes in the balance of various antagonistic control mechanisms.

383 Nonetheless, the herein described maintenance of Hsd11b1 expression at levels much lower than P0
384 level during septation period is novel and developmentally highly significant. Although in cell-free
385 system, this interconverting enzyme of cortisone and cortisol behaves mainly as a dehydrogenase

386 (inactivation), in vivo it is considered to perform 11β -reduction (activation) (10). Because
387 corticosteroids have been reported to inhibit septation and to terminate alveolarization through fusion
388 of the double capillary layer and thinning of septa (32, 43), low pulmonary corticosteroid activation
389 subsequent to low Hsd11b1 expression level therefore appears as requisite for septation. Pursued
390 elevation of Hsd11b1 expression between days 14 and 28 appears conversely to relate to
391 corticosteroid-driven septation arrest and maturation of septa.

392 Several issues could account for difficulty in interpreting FGF18-induced effects. In the lung, FGF18
393 is released by interstitial cells (3, 7, 51), and possibly endothelial cells (2). The use of SP-C regulatory
394 sequence to target FGF18 transgene expression on alveolar epithelial type II cells therefore leads to
395 ectopic expression. This might have changed local availability of the factor, and it cannot be ruled out
396 that this might have affected the responsiveness of its target cells, which could have been somehow
397 different from that to FGF18 expressed from endogenous gene. Also likely to be involved in possible
398 differences appear changes in cellular microenvironment, i.e. interaction of FGF18 with signal
399 molecules either different or present in different relative proportions in the pre- and postnatal lung.
400 Hence, paradoxical changes observed in double-transgenic pups might have been permitted by
401 conditions prevailing around birth that were different from those during alveolarization. In addition,
402 difficulties could be inherent to the model itself because of possible toxicity of the SP-C-rtTA
403 transgene and because doxycycline is a pan-MMP (matrix metalloproteinase) inhibitor while MMPs
404 play a functional role in alveolarization (discussed in 52). The absence of lung morphological changes
405 in developing (this study) or adult (51) mice of this strain however argues against this assumption.
406 Last, RT-qPCR post-hoc analysis gave more consistent results for up-regulated than for down-
407 regulated genes. This appeared to be due to wide random expression variations of genes that presented
408 by chance lower expression in those 4 double-transgenic lung samples used for microarray analysis.
409 Because it was indeed not possible to perform individual RT-qPCR control for all gene expressions
410 found to be diminished in microarray data, decreases were considered to be effective when there was
411 consistency for several genes among a group (e.g. cell-type markers or genes encoding products with
412 similar functions or involved in a same pathway). These considerations point the interest of examining

413 the developmental expression profile of putative target genes to interpret results from transcriptome
414 analysis.

415

416 **Adrenomedullin and genes involved in angiogenesis.**

417 The primary target of FGF18 was Adm gene, the expression of which was increased about 7-fold by
418 transgene induction. Adm developmental expression profile, which, similar to that of FGF18
419 displayed peak coincidental with secondary septation, was consistent with control by endogenous
420 FGF18. Adrenomedullin is hypoxia-inducible peptide with vasodilator, antioxidative and angiogenic
421 properties, highly expressed in the developing lung. Not only has Adm been reported to regulate cell
422 growth and survival, to induce proliferation and migration of endothelial progenitor cells, to enhance
423 the regenerating potential of the latter for pulmonary endothelium (36), and to regenerate alveoli and
424 vasculature in elastase-induced pulmonary emphysema (35), but its role in alveolar development was
425 recently evidenced (46). Lung expression of its transcript increases during alveolar development in rat
426 lung also, and Adm requirement for alveolar septation and angiogenesis was demonstrated in this
427 species (46). Whereas intranasal administration of an adrenomedullin-antagonist decreased lung
428 VEGF expression and capillary density, and impaired alveolar development, giving exogenous
429 adrenomedullin in a hyperoxic model of BPD reciprocally attenuated arrested lung angiogenesis and
430 alveolar development (46).

431 FGF18-transgene induction also enhanced expression of other genes likely to be involved in
432 angiogenesis, including Wnt2, a growth and differentiation factor for endothelial cells (22). This is
433 consistent with decreased Wnt2 expression reported in compound FGFR3/4 mutant mice (42).
434 Although more modestly, FGF18 also enhanced the expression of cullin 2 (not shown in table 4),
435 which is required for vascular development through regulation of VEGF transcription mediated by
436 hypoxia-inducible factor α (29).

437 The importance of FGF18 for angiogenesis had been evidenced previously in other organs by its
438 chemotactic effect for endothelial cells (1) and by delayed skeletal vascularization in FGF18^{-/-} mice
439 (27). Consistently, vessel size and PECAM labeling were increased in the lung of SP-C-rtTA/(teto)⁷⁻-
440 FGF18 mouse fetuses treated with doxycycline during whole gestation (51). Our findings now identify

441 FGF18 as a likely important player in the control of alveolar angiogenesis, an event that is absolute
442 requirement for alveolarization and is compromised in BPD.

443

444 **FGF18 effects related with cell migration.**

445 FGF18 is known to drive cell migration, especially for endothelial cells (1, 27), which is in keeping
446 with effects of FGF18 transgene on a panel of genes involved in this process. In addition to Adm,
447 these include the zinc-finger transcription factor-encoding genes Snai1 (Snail) and Snai2 (Slug), sushi
448 repeat protein, Lrps 1 and 2, and Nedd 9. However, in addition to promotion of cell movement during
449 organogenesis, SNAI proteins are also well known to be involved in epithelial-mesenchymal transition
450 (EMT) and metastatic invasion (37). In the lung, their overexpression was sufficient to induce EMT in
451 alveolar epithelial cells whereas SNAI depletion conversely attenuated TGF β 1-induced cell migration
452 and EMT (18). Up regulation of Wnt2 and down regulation of Sfrp1, both induced by FGF18, are also
453 involved in EMT (20). Although these FGF18 effects could therefore appear as favoring EMT, there is
454 no EMT during normal alveolar development. EMT is by contrast encountered in pathological
455 condition, namely lung fibrosis, via activation of endogenous latent TGF β 1 (21). Among other
456 possible mechanisms, prevention of EMT during alveolarization could be due to the simultaneous
457 induction of counteracting mechanisms by FGF18, including (i) down-regulation of genes encoding
458 factors involved in cell invasion and metastasis such as doublecortin (13), PAI1 and PAI2 (33), and
459 semaphorin 5A (40), and (ii) up-regulation of genes that inhibit spreading of mesenchyme-derived
460 cells including fibulin-1 (53) and FISP/IL24 (9).

461 Also consistent appears the FGF18-induced reduced expression of numerous muscle-cell markers,
462 which are expressed in the lung by smooth muscle cells and myofibroblasts. FGF18 thus reduced
463 notably the expression of genes that are known to be down-regulated at initiation of mouse lung
464 alveolarization (54), but were conversely up-regulated in TGF β 1-induced fibroblast-to-myofibroblast
465 transdifferentiation (44) or in experimental hyperoxia-induced BPD (47). Prostaglandin E2 has been
466 repeatedly reported to modulate lung inflammation and to prevent the fibroblast-to-myofibroblast
467 transition through E prostanoid receptor 2 (Ptger2) signal (23, 50). Taken together, the increased

468 number of pulmonary myofibroblasts in compound FGFR3/4 mutant mice (42) and the increased
469 expression of Ptger2 consecutive to FGF18 induction evidenced herein strongly argue for a
470 physiological role of FGF18 in prevention of fibrosis. Although myofibroblast differentiation and
471 migration are necessary to alveolarization (26), FGF18 might prevent these from becoming excessive
472 and falling over into EMT and fibrosis.

473

474

475 **Effects on ECM components.**

476 FGF18 strongly enhanced the expression of the ECM components bone sialoprotein, chondroitin
477 sulfate proteoglycans, and fibulin 1. Fibulin 1 is clearly indispensable to normal alveolar development
478 (24). The role of bone sialoprotein in alveolarization is unknown, but its expression peak coincidental
479 with secondary septation and its angiogenic properties (38) argue for involvement. As regards
480 chondroitin sulfate proteoglycans, they are known to be present in alveolar basement membrane.
481 FGF18 conversely decreased the expression of a variety of other ECM components. Previous
482 investigations (4, 31, 54) have evidenced clusters of ECM-component genes up regulated either early
483 during the phase of secondary septation or later during maturation of septa. FGF18 appears as an
484 inducer of genes belonging to the former group. Interestingly, the expression of the ECM-related
485 genes asporin and microfibrillar protein 5 that was increased in FGFR3/4-null mice (42) was
486 conversely decreased by FGF18 induction, suggesting that FGF18 decreases expression of the late-
487 group genes.

488

489 **Other effects.**

490 FGF18 enhanced the expression of a variety of cytochrome oxidases and of genes involved in
491 antioxidant mechanisms. The postnatal developmental expression profiles of glutathione-S-transferase
492 and ceruloplasmin, with high postnatal level and fall on day 14, were consistent with control by
493 FGF18. This is interesting in a therapeutic perspective, because preterm infants have immature
494 antioxidant defense mechanisms and increased susceptibility to oxidative stress, which in turn is
495 precipitating factor of BPD. Conversely, FGF18 down regulated a number of P450 cytochrome
496 oxidases and other genes involved in xenobiotic metabolism. Numerous cytochrome oxidases with
497 FGF18-decreased expression, including Cyp2b10, Cyp2b20, Cyp2f2 and Cyp4b1 were recently found
498 to be down regulated in the alveolarizing postnatal lung (54). It was suggested that these changes
499 could be related to expansion of epithelial precursor cell pool through balance between proliferation
500 and differentiation of epithelial cells (54). Consistent with this assumption is the FGF18-diminished
501 expression of a number of genes expressed selectively in lung epithelial cell subsets, including Ca⁽²⁺⁾-
502 sensitive chloride channel 2, Abca3, Cyp1b1, Cyp2f2, stearyl coenzyme A dehydrogenase (Scd1),

503 aquaporins 3 and 4, uteroglobin-related protein 1a, and aldehyde oxidase 3. However, targeting the
504 expression of FGF18 transgene on type II cells by the use of SP-C promoter might have enhanced
505 these effects.

506 Lastly, it is worth pointing that, although not consistent with a negative control by endogenous
507 FGF18, the developmental expression profile of Crabp1 remarkably presents a peak coincidental with
508 alveolar septation. Taking into account the central role of RA released by lipofibroblasts in
509 alveolarization (5), this appears to correspond to maximal capacity of lung cells to link and retain RA.

510

511 **Acknowledgments**

512 SP-C-rtTA-FGF-18 founder mice were obtained from the Cincinnati Children's Research Foundation
513 through material transfer agreement established on October 28, 2003.

514 REFERENCES

515

516 1. **Antoine M, Wirz W, Tag CG, Gressner AM, Wycislo M, Muller R, and Kiefer P.**
517 Fibroblast growth factor 16 and 18 are expressed in human cardiovascular tissues and induce
518 on endothelial cells migration but not proliferation. *Biochem Biophys Res Commun* 346: 224-
519 233, 2006.

520 2. **Antoine M, Wirz W, Tag CG, Mavituna M, Emans N, Korff T, Stoldt V,**
521 **Gressner AM, and Kiefer P.** Expression pattern of fibroblast growth factors (FGFs), their
522 receptors and antagonists in primary endothelial cells and vascular smooth muscle cells.
523 *Growth Factors* 23: 87-95, 2005.

524 3. **Boucherat O, Benachi A, Barlier-Mur AM, Franco-Montoya ML, Martinovic J,**
525 **Thebaud B, Chailley-Heu B, and Bourbon JR.** Decreased lung fibroblast growth factor 18
526 and elastin in human congenital diaphragmatic hernia and animal models. *Am J Respir Crit*
527 *Care Med* 175: 1066-1077, 2007.

528 4. **Boucherat O, Franco-Montoya ML, Thibault C, Incitti R, Chailley-Heu B,**
529 **Delacourt C, and Bourbon JR.** Gene expression profiling in lung fibroblasts reveals new
530 players in alveolarization. *Physiol Genomics* 32: 128-141, 2007.

531 5. **Bourbon J, Delacourt C, and Boucherat O.** Basic mechanisms of alveolarization.
532 *In: Abman SH, editor, Bronchopulmonary dysplasia New York: Informa Healthcare* p.56-88,
533 2009.

534 6. **Bourbon JR, Boucherat O, Boczkowski J, Crestani B, and Delacourt C.**
535 Bronchopulmonary dysplasia and emphysema: in search of common therapeutic targets.
536 *Trends Mol Med* 15: 169-179, 2009.

537 7. **Chailley-Heu B, Boucherat O, Barlier-Mur AM, and Bourbon JR.** FGF-18 is
538 upregulated in the postnatal rat lung and enhances elastogenesis in myofibroblasts. *Am J*
539 *Physiol Lung Cell Mol Physiol* 288: L43-51, 2005.

540 8. **Chailley-Heu B, Boucherat O, Benachi A, Bourbon JR.** FGF18 is up-regulated at
541 the onset of alveolar septation in rodent and human lungs. *Proc. Am Thor Soc* 2006; 3:A674.

542 9. **Chen J, Chada S, Mhashilkar A, and Miano JM.** Tumor suppressor MDA-7/IL-24
543 selectively inhibits vascular smooth muscle cell growth and migration. *Mol Ther* 8: 220-229,
544 2003.

545 10. **Draper N, and Stewart PM.** 11beta-hydroxysteroid dehydrogenase and the pre-
546 receptor regulation of corticosteroid hormone action. *J Endocrinol* 186: 251-271, 2005.

547 11. **Elluru RG, Thompson F, and Reece A.** Fibroblast growth factor 18 gives growth
548 and directional cues to airway cartilage. *Laryngoscope* 119: 1153-1165, 2009.

549 12. **Eswarakumar VP, Lax I, and Schlessinger J.** Cellular signaling by fibroblast
550 growth factor receptors. *Cytokine Growth Factor Rev* 16: 139-149, 2005.

551 13. **Feng Y, and Walsh CA.** Protein-protein interactions, cytoskeletal regulation and
552 neuronal migration. *Nat Rev Neurosci* 2: 408-416, 2001.

553 14. **Hyatt BA, Shangquan X, and Shannon JM.** BMP4 modulates fibroblast growth
554 factor-mediated induction of proximal and distal lung differentiation in mouse embryonic
555 tracheal epithelium in mesenchyme-free culture. *Dev Dyn* 225: 153-165, 2002.

556 15. **Ihaka R, and Gentleman R.** R: a language for data analysis and graphics. *Comput*
557 *Graph Stat* 5: 299-314, 1996.

558 16. **Irizarry RA, Gautier L, and Cope L.** An R package for analysis of Affymetrix
559 oligonucleotide arrays. *In: The analysis of Gene Expression Data: Methods and Software:*
560 *Methods and software, edited by Parmigiani G, Garrett ES, Irizarry SA, Zeger SL New York:*
561 *Springer* 2002.

- 562 17. **Irizarry RA, Hobbs B, Collin F, Beazer-Barclay YD, Antonellis KJ, Scherf U,**
563 **and Speed TP.** Exploration, normalization, and summaries of high density oligonucleotide
564 array probe level data. *Biostatistics* 4: 249-264, 2003.
- 565 18. **Jayachandran A, Konigshoff M, Yu H, Rupniewska E, Hecker M, Klepetko W,**
566 **Seeger W, and Eickelberg O.** SNAI transcription factors mediate epithelial-mesenchymal
567 transition in lung fibrosis. *Thorax* 64: 1053-1061, 2009.
- 568 19. **Jobe AH, Bancalari E.** Bronchopulmonary dysplasia. *Am J Respir Crit Care Med*
569 163: 1723-1729, 2001.
- 570 20. **Kato M.** Epithelial-mesenchymal transition in gastric cancer (Review). *Int J Oncol*
571 27: 1677-1683, 2005.
- 572 21. **Kim KK, Kugler MC, Wolters PJ, Robillard L, Galvez MG, Brumwell AN,**
573 **Sheppard D, and Chapman HA.** Alveolar epithelial cell mesenchymal transition develops in
574 vivo during pulmonary fibrosis and is regulated by the extracellular matrix. *Proc Natl Acad*
575 *Sci U S A* 103: 13180-13185, 2006.
- 576 22. **Klein D, Demory A, Peyre F, Kroll J, Augustin HG, Helfrich W, Kzhyshkowska**
577 **J, Schledzewski K, Arnold B, and Goerdts S.** Wnt2 acts as a cell type-specific, autocrine
578 growth factor in rat hepatic sinusoidal endothelial cells cross-stimulating the VEGF pathway.
579 *Hepatology* 47: 1018-1031, 2008.
- 580 23. **Kolodick JE, Peters-Golden M, Larios J, Toews GB, Thannickal VJ, and Moore**
581 **BB.** Prostaglandin E2 inhibits fibroblast to myofibroblast transition via E. prostanoid receptor
582 2 signaling and cyclic adenosine monophosphate elevation. *Am J Respir Cell Mol Biol* 29:
583 537-544, 2003.
- 584 24. **Kostka G, Giltay R, Bloch W, Addicks K, Timpl R, Fassler R, and Chu ML.**
585 Perinatal lethality and endothelial cell abnormalities in several vessel compartments of
586 fibulin-1-deficient mice. *Mol Cell Biol* 21: 7025-7034, 2001.
- 587 25. **Li C, and Wong WH.** Model-based analysis of oligonucleotide arrays: expression
588 index computation and outlier detection. *Proc Natl Acad Sci U S A* 98: 31-36, 2001.
- 589 26. **Lindahl, P Karlsson R, Hellstrom M, Gebre-Medhin S, Willets K, Heath JK,**
590 **Betsholtz C.** Alveogenesis failure in PDGF-A-deficient mice is coupled to lack of distal
591 spreading of alveolar smooth muscle cell progenitors during lung development. *Development*
592 124: 3943-3953, 1997.
- 593 27. **Liu Z, Lavine KJ, Hung IH, and Ornitz DM.** FGF18 is required for early
594 chondrocyte proliferation, hypertrophy and vascular invasion of the growth plate. *Dev Biol*
595 302: 80-91, 2007.
- 596 28. **Lopez E, Boucherat O, Franco-Montoya ML, Bourbon JR, Delacourt C, and**
597 **Jarreau PH.** Nitric oxide donor restores lung growth factor and receptor expression in
598 hyperoxia-exposed rat pups. *Am J Respir Cell Mol Biol* 34: 738-745, 2006.
- 599 29. **Maeda Y, Suzuki T, Pan X, Chen G, Pan S, Bartman T, and Whitsett JA.** CUL2
600 is required for the activity of hypoxia-inducible factor and vasculogenesis. *J Biol Chem* 283:
601 16084-16092, 2008.
- 602 30. **Mariani T.** Regulation of alveogenesis by reciprocal proximodistal fibroblast growth
603 factor and retinoic acid signaling. *Am J Respir Cell Mol Biol* 31: S52-S57, 2004.
- 604 31. **Mariani TJ, Reed JJ, and Shapiro SD.** Expression profiling of the developing
605 mouse lung: insights into the establishment of the extracellular matrix. *Am J Respir Cell Mol*
606 *Biol* 26: 541-548, 2002.
- 607 32. **Massaro D, Massaro GD.** Dexamethasone accelerates postnatal alveolar wall
608 thinning and alters wall composition. *Am J Physiol Regul Integr Comp Physiol* 251: R218-
609 R224, 1986.
- 610 33. **McMahon B, and Kwaan HC.** The plasminogen activator system and cancer.
611 *Pathophysiol Haemost Thromb* 36: 184-194, 2008.

- 612 34. **Mesas-Burgos C, Nord M, Didon L, Eklof AC, and Frenckner B.** Gene expression
613 analysis after prenatal tracheal ligation in fetal rat as a model of stimulated lung growth. *J*
614 *Pediatr Surg* 44: 720-728, 2009.
- 615 35. **Murakami S, Nagaya N, Itoh T, Iwase T, Fujisato T, Nishioka K, Hamada K,**
616 **Kangawa K, and Kimura H.** Adrenomedullin regenerates alveoli and vasculature in
617 elastase-induced pulmonary emphysema in mice. *Am J Respir Crit Care Med* 172: 581-589,
618 2005.
- 619 36. **Nagaya N, Mori H, Murakami S, Kangawa K, and Kitamura S.** Adrenomedullin:
620 angiogenesis and gene therapy. *Am J Physiol Regul Integr Comp Physiol* 288: R1432-1437,
621 2005.
- 622 37. **Nieto MA.** The snail superfamily of zinc-finger transcription factors. *Nat Rev Mol*
623 *Cell Biol* 3: 155-166, 2002.
- 624 38. **Ogata Y.** Bone sialoprotein and its transcriptional regulatory mechanism. *J*
625 *Periodontal Res* 43: 127-135, 2008.
- 626 39. **Olsen SK, Li JY, Bromleigh C, Eliseenkova AV, Ibrahim OA, Lao Z, Zhang F,**
627 **Linhardt RJ, Joyner AL, and Mohammadi M.** Structural basis by which alternative
628 splicing modulates the organizer activity of FGF8 in the brain. *Genes Dev* 20: 185-198, 2006.
- 629 40. **Pan GQ, Ren HZ, Zhang SF, Wang XM, and Wen JF.** Expression of semaphorin
630 5A and its receptor plexin B3 contributes to invasion and metastasis of gastric carcinoma.
631 *World J Gastroenterol* 15: 2800-2804, 2009.
- 632 41. **Powell PP, Wang CC, Horinouchi H, Shepherd K, Jacobson M, Lipson M, and**
633 **Jones R.** Differential expression of fibroblast growth factor receptors 1 to 4 and ligand genes
634 in late fetal and early postnatal rat lung. *Am J Respir Cell Mol Biol* 19: 563-572, 1998.
- 635 42. **Srisuma S, Bhattacharya S, Simon DM, Solleti SK, Tyagi S, Starcher B, and**
636 **Mariani TJ.** Fibroblast growth factor receptors control epithelial-mesenchymal interactions
637 necessary for alveolar elastogenesis. *Am J Respir Crit Care Med* 181: 838-850, 2010.
- 638 43. **Tschanz SA, Damke BM, Burri PH.** Influence of postnatally administered
639 glucocorticoids on rat lung growth. *Biol Neonate* 68: 229-245, 1995.
- 640 44. **Untergasser G, Gander R, Lilg C, Lepperdinger G, Plas E, and Berger P.**
641 Profiling molecular targets of TGF-beta1 in prostate fibroblast-to-myofibroblast
642 transdifferentiation. *Mech Ageing Dev* 126: 59-69, 2005.
- 643 45. **Usui H, Shibayama M, Ohbayashi N, Konishi M, Takada S, and Itoh N.** Fgf18 is
644 required for embryonic lung alveolar development. *Biochem Biophys Res Commun* 322: 887-
645 892, 2004.
- 646 46. **Vadivel A, Abozaid S, van Haaften T, Sawicka M, Eaton F, Chen M, and**
647 **Thebaud B.** Adrenomedullin promotes lung angiogenesis, alveolar development, and repair.
648 *Am J Respir Cell Mol Biol* 43: 152-160, 2009.
- 649 47. **Wagenaar GT, ter Horst SA, van Gastelen MA, Leijser LM, Mauad T, van der**
650 **Velden PA, de Heer E, Hiemstra PS, Poorthuis BJ, and Walther FJ.** Gene expression
651 profile and histopathology of experimental bronchopulmonary dysplasia induced by
652 prolonged oxidative stress. *Free Radic Biol Med* 36: 782-801, 2004.
- 653 48. **Weibel ER, Cruz-Orive LM.** Morphometric methods. In: *Crystal G & West JB,*
654 *editors, The Lung: Scientific Foundations (2nd ed.), Philadelphia: Raven p.333-344, 1997.*
- 655 49. **Weinstein M, Xu X, Ohyama K, and Deng CX.** FGFR-3 and FGFR-4 function
656 cooperatively to direct alveogenesis in the murine lung. *Development* 125: 3615-3623, 1998.
- 657 50. **White KE, Ding Q, Moore BB, Peters-Golden M, Ware LB, Matthay MA, and**
658 **Olman MA.** Prostaglandin E2 mediates IL-1beta-related fibroblast mitogenic effects in acute
659 lung injury through differential utilization of prostanoid receptors. *J Immunol* 180: 637-646,
660 2008.

- 661 51. **Whitsett JA, Clark JC, Picard L, Tichelaar JW, Wert SE, Itoh N, Perl AK, and**
662 **Stahlman MT.** Fibroblast growth factor 18 influences proximal programming during lung
663 morphogenesis. *J Biol Chem* 277: 22743-22749, 2002.
- 664 52. **Whitsett JA, and Perl AK.** Conditional control of gene expression in the respiratory
665 epithelium: A cautionary note. *Am J Respir Cell Mol Biol* 34: 519-520, 2006.
- 666 53. **Williams SA, and Schwarzbauer JE.** A shared mechanism of adhesion modulation
667 for tenascin-C and fibulin-1. *Mol Biol Cell* 20: 1141-1149, 2009.
- 668 54. **Wolff JC, Wilhelm J, Fink L, Seeger W, and Voswinckel R.** Comparative gene
669 expression profiling of post-natal and post-pneumonectomy lung growth. *Eur Respir J* 35:
670 655-666, 2010.
- 671 55. **Workman C, Jensen LJ, Jarmer H, Berka R, Gautier L, Nielser HB, Saxild HH,**
672 **Nielsen C, Brunak S, and Knudsen S.** A new non-linear normalization method for reducing
673 variability in DNA microarray experiments. *Genome Biol* 3: research0048, 2002.
- 674
- 675

676 **Figure legends**

677 Fig. 1. Experimental protocol for doxycycline treatment and lung sample collection. In order to induce
678 precocious expression of FGF18, advanced as compared with endogenous peak, transgenic SP-C-
679 rtTA- and (teto)₇-FGF18-mice were bred, and their progeny (gathering both single and double
680 transgenic individuals, and rarely wild type individuals) was treated by the inducer doxycycline.
681 Pregnant mice received first doxycycline in drinking water (0.5mg/ml) for the 2 last prenatal days.
682 Doxycycline was removed from drinking water on the day of birth (designated postnatal day 0 or P0),
683 and pups received then one daily subcutaneous injection of doxycycline aqueous solution 3 mg/ml (20
684 mg/kg bw) on P0, P1 and P2. Their lungs were collected on P3 and kept at -80°C until RNA extraction
685 for gene-expression analyses, or on P4, P8 or P16 for lung fixation and morphological/morphometric
686 analyses. Post-hoc genotyping of the pups was performed on DNA extracted from tail fragment.

687

688 Fig. 2. Semi-quantitative RT-PCR analysis of (teto)₇-FGF18 transgene expression in the 8 mouse pup
689 lung samples used for microarray hybridization. Transgene-specific primers were used as stated in
690 M&M, 25 amplification cycles were run. Lane 1, molecular-size ladder; lane 2, sample D4, SP-C-
691 rtTA/(teto)₇-FGF18 (double transgenic), litter 1; lane 3, sample D2, (teto)₇-FGF18 (single-transgenic
692 control), litter 1; lane 4, sample D34, SP-C-rtTA/(teto)₇-FGF18, litter 2; lane 5, sample D40, (teto)₇-
693 FGF18, litter 2; lane 6, sample D48, SP-C-rtTA/(teto)₇-FGF18, litter 3; lane 7, sample D50, (teto)₇-
694 FGF18, litter 3; lane 8, sample D52, SP-C-rtTA/(teto)₇-FGF18, litter 4; lane 9, sample D58, (teto)₇-
695 FGF18, litter 4. FGF18-transgene expression was manifest in double-transgenic pups bearing both the
696 inducible FGF18 transgene and the activator construct whereas it was not or barely detectable in their
697 littermates bearing only the FGF18 transgene.

698

699 Fig. 3. Morphological aspects of mouse lungs on postnatal day 4. Pups were issued from a same litter
700 and were treated by doxycycline as stated in M&M and Fig. 1. Lungs were collected on P4 that
701 revealed as the earliest stage for adequate pressure fixation in this species. Lungs were fixed with
702 paraformaldehyde at constant pressure, embedded in paraffin, cut at 4μm and stained by picro-indigo-

703 carmine. A. Wild-type mouse pup. B double-transgenic pup (SP-C-rtTA/(teto)₇-FGF18). C. Single-
704 transgenic pup ((teto)₇-FGF18). Morphology was similar in the 3 instances.

705

706 Fig. 4. Developmental expression profile from birth to adulthood in wild-type mouse lung of 11 genes
707 with expression found to be increased by FGF18-transgene induction in microarray analysis.
708 Quantitative RT-qPCR was used to determine expression levels. Endogenous-FGF18 expression
709 profile is also displayed for facilitating comparisons. Mean \pm se on 4 individual lung samples from 2
710 different litters per stage (absence of error bar means that it was too small to be represented at this
711 scale). Multiple stage comparison was made by Kruskal-Wallis analysis, followed by two-stage
712 comparisons by Mann and Whitney U test. To avoid overloading of the graphs, significant differences
713 are not represented, but significant changes are detailed in text. Gene symbols: Adm, adrenomedullin;
714 Hsd11b1, hydroxysteroid 11 β dehydrogenase 1; Gstm5, glutathione-S transferase, mu5; Wnt2,
715 wingless-related MMTV integration site 2, Snai, snail homolog, Ptger2, prostaglandin R receptor EP2
716 subtype.

717

718 Fig. 5. Developmental expression profile from birth to adulthood in wild-type mouse lung of 6 genes
719 with expression found to be decreased by FGF18-transgene induction in microarray analysis.
720 Quantitative RT-qPCR was used to determine expression levels. Mean \pm se on 4 individual lung
721 samples from 2 different litters per stage (absence of error bar means that it was too small to be
722 represented at this scale). Multiple stage comparison was made by Kruskal-Wallis analysis, followed
723 by two-stage comparisons by Mann and Whitney U test. To avoid overloading of the graphs,
724 significant differences are not represented, but significant changes are detailed in text. Gene symbols:
725 C1qtnf3, C1q and tumor necrosis factor related protein 3; Scd1, stearyl-coenzyme A desaturase 1;
726 Abca3, ATP-binding cassette transporter ABCA3; Dcx, doublecortin, Crabp1, cellular retinoic acid
727 binding protein 1; Cyp1b1, cytochrome P450, 1b1.

728

729 Table 1. *Sequence of primers used for RT-qPCR determinations*

730

Gene name (official symbol; accession number)	Forward primer (5'-3')	Reverse primer (5'-3')
Fibroblast growth factor 18 (FGF18; NM_008005)	TGAACACGCACTCCTTGCTAGT	GAATTCTACCTGTGTATGAACCGAAA
Adrenomedullin (Adm; NM_009627)	GAAGGACTTCTTTCTGCTTCAAGTG	GCGAGTGAACCAATAACATCA
CD36 antigen (cd36; NM_007643)	GCAAAGTTGCCATAATTGAGTCTCA	CTGCGTCTGTGCCATTAATCA
Hydroxysteroid 11-beta dehydrogenase 1 (Hsd11b1; NM_007643)	TCTCTGTGTCCTTGGCCTCATA	CACTCCTCCTGGGAGAAGCT
Bone sialoprotein (Ibsp1; NM_008318)	CATGCCTACTTTTATCCTCCTCTGA	AACTATCGCCGCTCCATTTTC
Glutathione S transferase mu5 (Gstm5; NM_010360)	GGACGTGAAATCAAGCTAGATCTG	CTTGTTCTTCCCGTCCATGAG
Ceruloplasmine (Cp; NM_007752)	TGCTGGGATGGCAACTACCT	CGTTTTCCACTTATCGCCAATF
Wingless-related MMTV integration site 2 (Wnt2; NM_023653)	CTGGACAGAGATCACAGCCTCTT	GCGTAAACAAAGGCCGATTC
Snail homolog 2 (Snai2; NM_011415)	AAGCCCAACTACAGCGAACTG	CGAGGTGAGGATCTCTGGTTTT
Fibulin 1 (Fbln1; NM_010180)	ACCAAGAAGACCCGTACCTGAA	GTCACGGCACTGCTGCTTAC
Prostaglandin E receptor EP2 subtype (Ptger2; NM_008964)	GCCTTTCACAATCTTTGCCTACAT	GACCGGTGGCCTAAGTATGG
Snail homolog 1 (Snai1; NM_011427)	GGGCGCTCTGAAGATGCA	GTTGGAGCGGTGAGCAAAAAG
Clq and tumor necrosis factor related protein 3 (Clqtnf3; NM_030888)	GCACAACGGCAACACAGTCT	TGCATGGTTGCTGGATGTATC
StearoylCoA desaturase 1 (Scd1; NM_009127)	CCATGCAGGCAGGTAGTGGTA	TGCCCATGTCTCTGGTGTITTA
ATP-binding cassette transporter 3 (ABCA3; AY083616)	AGCCAACATAGCAGCAGCC	TACCGAGGAGCCACGAAAAA
Osteoglycin (Ogn; NM_008760)	CAGATGATACATTCTGCAAGGCTAA	CCTCCAGGCGAATCTCTTCA
Fibroblast activation protein (Fap; NM_007986)	TGATTCTGCCTCCTCAGTTTGA	CAGACTTAACACTCTGGCTGCAA
Doublecortin (Dcx; NM_010025)	AAAAACTCTACACCTTGATGGAAA	TGCATTCAATCTCATCCAAGGA
Cellular retinoic acid binding protein 1 (Crabp1; NM_013496)	GGGCTTCGAGGAGGAGACA	TGTGCAGTGAATCTTGTCTCATTC
SRY-box containing gene (Sox2; NM_011443)	AGATGCACAACCTCGGAGATCAG	GCTTCTCGGTCTCGGACAAA
Aldehyde dehydrogenase 1, subfamily A1 (Aldh1a1; NM_013467)	GGCTCTCACCTGGCATCTTT	CCCATAACCAGGGACAATGTTT
Cytochrome P450, 1b1 (Cyp1b1; NM_009994)	AGGTTGAAGCCTTGCCAGAA	TGCTGTGGACTGTCTGCACTAA

731

732

733 Table 2. *Evaluation of quality filter criteria in microarrays*

734

Sample	Scale factor	% P	Ratio 3'/5' actin	Ratio 3'/5' GAPDH
(validation threshold)	Max/Min<3	>20 and Max-Min<15	<4	<4
D2-C	0.504	60.4	1.25	0.77
D4-DT	0.582	59.5	1.30	0.93
D34-C	0.661	59.3	1.26	0.74
D40-DT	0.643	60.7	1.25	0.87
D48-C	0.635	60.6	1.25	0.78
D50-DT	0.486	60.8	1.25	0.81
D52-C	0.544	60.2	1.25	0.76
D58-DT	0.606	60.0	1.27	0.77
Mean ± se	0.580 ± 0.023	60.19 ± 0.20	1.26 ± 0.006	0.804 ± 0.004

735

736

737

738

739

740

741

742

743

744

Table 3. *Morphometric analysis of the lungs of doxycycline-treated pups*

745

746

n	P4		P8		P16	
	controls	double transgenic	controls	double transgenic	controls	double transgenic
	10	9	8	8	14	8
VL (cm ³)	0.135 ± 0.009	0.152 ± 0.010	0.249 ± 0.014	0.271 ± 0.017	0.376 ± 0.015	0.392 ± 0.027
Sva (cm ² /cm ³)	294 ± 12	277 ± 10	340 ± 18	293 ± 17	361 ± 12	358 ± 17
Vvp (%)	0.964 ± 0.007	0.986 ± 0.019	0.989 ± 0.002	0.992 ± 0.002	0.995 ± 0.001	0.992 ± 0.002
MLI (µm)	13.8 ± 0.5	14.6 ± 0.5	12.0 ± 0.7	14.0 ± 0.8	11.3 ± 0.4	11.3 ± 0.5
Sa (cm ²)	38 ± 3	41 ± 2	83 ± 6	79 ± 7	135 ± 7	139 ± 10

747

748

749

750

751

752

753

754

Treatment with doxycycline was the same as that for animals used for microarray analysis. Pups were collected from 3 or 4 litters per stage at postnatal days 4, 8 or 16. Data are mean ± SE. Abbreviations: n, number of individuals per group; VL, lung volume; Sva, alveolar surface density; Vvp, volumetric density of lung alveolar parenchyma; MLI, mean linear intercept; Sa, absolute surface area of airspaces. No significant difference was observed between the 2 groups for any parameter either at P4, P8 or P16 (two-tailed *t*-test).

755 Table 4. Results of array analysis: genes up regulated at least 25%* by FGF18 induction in the 4
 756 double-transgenic mouse pups as compared to their respective littermate single-transgenic controls
 757 (one-tailed paired t test).
 758

Accession #	Name	Funct. Cat.	log2-fold change	fold change	P value
NM_009627	adrenomedullin (Adm)	Signal, Angio	2.02628	x 4.074	0.0494
NM_007643	CD36 antigen	Lmetab+Antifib	1.06464	x 2.092	0.0463
NM_008288	hydroxysteroid 11-beta dehydrogenase 1 (Hsd11b1)	Enz, Ster metab	1.00447	x 2.0	0.0364
NM_008318	bone sialoprotein (integrin-binding sialoprotein, IBSP)	ECM+Recept	0.83998	x 1.79	0.014
NM_010360	glutathione S-transferase, mu 5 (Gstm5)	Enz, Antiox	0.75917	x 1.693	0.0379
NM_007752	ceruloplasmin (Cp)	Enz, Antiox	0.72622	x 1.654	0.0393
NM_023653	wingless-related MMTV integration site 2 (Wnt2)	Signal, Angio+Migr	0.58788	x 1.5	0.0357
NM_029796	leucine-rich alpha-2-glycoprotein 1 (Lrg1)	Antiox	0.55743	x 1.472	0.0028
NM_021282	cytochrome P450, 2e1, ethanol inducible (Cyp2e1)	Enz, Antiox	0.55580	x 1.47	0.0305
BI964347	a disintegrin and metalloproteinase domain 12 (meltrin alpha)	Enz, ECM	0.54291	x 1.457	0.0283
NM_033037	cysteine dioxygenase 1, cytosolic (Cdo1)	Enz, Antiox	0.51247	x 1.426	0.037
AF333251	Th2-specific cytokine FISP/IL24	Signal, Antifib	0.48965	x 1.4	0.0417
NM_010023	dodecenoyl-Coenzyme A delta isomerase (Dci)	Enz, Lmetab	0.48113	x 1.4	0.0077
C77655	CD84 antigen	Immun	0.46537	x 1.381	0.0311
NM_011415	snail homolog 2 (Drosophila) (Snai2)	Signal, Migr+EMT	0.45841	x 1.374	0.0412
NM_010180	fibulin 1 (Fbln1)	ECM+Antifib	0.45225	x 1.368	0.0354
BB131147	Borg4-pending /binder of Rho GTPase 4	Recept, Antifib	0.44920	x 1.365	0.0261
BQ176864	protein phosphatase 1, regulatory (inhibitor) subunit 3C (Ppp1r3c)	Enz, Glyc metab	0.43991	x 1.357	0.0408
BC028307	Similar to sushi-repeat protein	Migr	0.43074	x 1.348	0.0257
NM_010717	LIM-domain containing, protein kinase (Limk1)	Enz, Antifib	0.42335	x 1,341	0,006
NM_011146	peroxisome proliferator activated receptor gamma (Pparg)	Signal, Lmetab	0.41266	x 1.331	0.0425
NM_008118	gastric intrinsic factor (Gif)	Transport	0.38563	x 1.306	0.0403
NM_008059	G0G1 switch gene 2 (G0s2)	Prolif	0.37920	x 1.3	0.0334
X14607	lipocalin 2 / Mouse SV-40 induced 24p3 mRNA	Migr	0.35332	x 1.277	0.0197
NM_011611	tumor necrosis factor receptor superfamily, member 5 (Tnfrsf5)	Signal, Immun	0.33640	x 1.263	0.0425
NM_023323	brix domain containing 1 (Bxdc1)	Prolif	0.33067	x 1.258	0.0237
BC008277	Similar to Endothelin receptor type A	Recept, Angio	0.32332	x 1.251	0.0207
NM_008964	prostaglandin E receptor EP2 subtype (Ptger2)	Recept, Antifib	0.31244	x 1.242	0.0427
NM_019389	chondroitin sulfate proteoglycan 2 (Cspg2)	ECM	0.30793	x 1.238	0.0234
NM_080849	NIMA-related expressed kinase 8 (Nek8)	Enz, Prolif	0.29273	x 1.225	0.0356
NM_007996	adrenodoxin	Antiox	0.29229	x 1.225	0.0264
NM_011427	snail homolog 1, (Drosophila) (Snai1)	Signal, Migr+EMT	0.29147	x 1.224	0.0213

759 *Five genes of interest increased 22.4 to 24.2% have been added to the list.

760 Abbreviations: Funct. Cat., functional category of gene product; Angio, angiogenesis; Antifib, anti-fibrotic effects; Antiox,
 761 anti-oxidant metabolism; ECM, extracellular-matrix component or metabolism; EMT, epithelial-mesenchymal transition;
 762 Enz, enzyme or enzyme inhibitor; Glyc metab, glycogene megtabolism; Immun, immune system; Lmetab, lipid metabolism;
 763 Migr, cell migration; Prolif, cell proliferation; Recept, receptor; Signal, signaling molecule; Ster metab, steroid metabolism;
 764 Transport, transporter molecule.

765 Genes with name and symbol in bold character had changes checked by RT-qPCR.
 766
 767

768
769
770
771

Table 5. Results of array analysis: genes down regulated at least 25% by FGF18 induction in the 4 double-transgenic mouse pups as compared to their respective littermate single-transgenic controls (one-tailed paired t test).

Accession #	Name	Funct. Cat.	log2-fold change	fold change	P value
NM_030888	Clq and tumor necrosis factor related protein 3 (Clqtnf3/cartonectin)	Signal, Lipog	-1.59897	x 0.33	0.0094
NM_030601	Ca(2+)-sensitive chloride channel 2 (Cacc)	Transport, Epm	-1.39070	x 0.381	0.0039
NM_009127	stearoyl-Coenzyme A desaturase 1 (Scd1)	Enz, Lipog	-1.28176	x 0.411	0.0088
AY083616	ATP-binding cassette transporter ABCA3	Transport, Epm	-1.05604	x 0.481	0.0004
NM_008760	osteoglycin (Ogn)	ECM	-1.04551	x 0.484	0.0088
NM_007986	fibroblast activation protein (Fap/seprase)	Enz, ECM, Migr	-1.02764	x 0.491	0.0002
AK007703	homolog to ATP-binding cassette transporter, sub-family A, member 3	Transport, Epm	-0.97681	x 0.508	0.0003
NM_010025	doublecortin	Migr	-0.94387	x 0.52	0.0103
NM_021400	proteoglycan 4 (Prg4)	ECM	-0.92209	x 0.528	0.0187
NM_009181	sialyltransferase 8 (alpha-2, 8-sialyltransferase) B (Siat8b)	Enz, Glycoconj	-0.89706	x 0.537	0.0265
NM_009608	actin, alpha, cardiac (Actc1)	MCm	-0.88653	x 0.541	0.0397
NM_009393	troponin C, cardiac/slow skeletal (Tnnc1)	MCm	-0.86216	x 0.55	0.0262
NM_013496	cellular retinoic acid binding protein I (Crabp1)	Retino metab	-0.85952	x 0.551	0.0373
NM_011674	UDP-glucuronosyltransferase 8	Enz, Detox	-0.82905	x 0.563	0.0247
NM_013808	cysteine-rich protein 3 (Csrp3)	MCm	-0.80843	x 0.571	0.0064
NM_010867	myomesin 1 (Myom1)	MCm	-0.79768	x 0.575	0.0049
AF311699	c-type lectin protein MT75 (chondrolectin)	ECM	-0.79070	x 0.578	0.0003
NM_015825	SH3-binding domain glutamic acid-rich protein (Sh3bgr)	MCm	-0.78637	x 0.581	0.0121
NM_033268	actinin alpha 2 (Actn2)	MCm	-0.77289	x 0.585	0.0405
NM_013834	secreted frizzled-related sequence protein 1 (Sfrp1)	Prolif, EMT	-0.76298	x 0.589	0.0005
NM_010858	myosin light chain, alkali, cardiac atria (Myla)	MCm	-0.75605	x 0.592	0.0373
NM_018870	phosphoglycerate mutase 2 (Pgam2)	Enz, Inter metab	-0.74443	x 0.597	0.0268
NM_011620	troponin T3, skeletal, fast (Tnnt3)	MCm	-0.73578	x 0.6	0.0170
NM_011443	high mobility group box protein (SRY-box containing gene 2, Sox2)	Transcrip, Epm	-0.72852	x 0.6	0.0028
NM_013467	aldehyde dehydrogenase family 1, subfamily A1 (Aldh1a1)	Retino metab	-0.71960	x 0.607	0.0216
NM_011111	plasminogen activator inhibitor, type II (Serpinb2)	Signal, Migr	-0.71960	x 0.607	0.0019
NM_016689	aquaporin-3	Transport, Epm	-0.69277	x 0.619	0.0330
NM_009944	cytochrome c oxidase subunit VIIa-H precursor (Cox7ah)	Enz, Detox	-0.68876	x 0.62	0.0211
NM_011395	solute carrier family 22 (organic cation transporter), member 3 (Slc22a3)	Transp	-0.68500	x 0.622	0.0149
NM_010856	Mouse alpha cardiac myosin heavy chain (Myhca)	MCm	-0.67333	x 0.627	0.0422
NM_009922	calponin 1 (Cnn1)	MCm	-0.66432	x 0.631	0.0093
BB193413	aquaporin 4 (Aqp4)	Transport, Epm	-0.65006	x 0.637	0.0335
AF274959	uteroglobin related protein 1A / secretoglobin (Scgb3a2)	Transport, Epm	-0.64771	x 0.638	0.0196
NM_008973	pleiotrophin	Sign	-0.64583	x 0.639	0.0007
AF128849	cytochrome P450 2B10 related protein (Cyp2b20)	Enz, Detox	-0.63401	x 0.644	0.0318
NM_010356	glutathione S-transferase, alpha 3 (Gsta3)	Enz, Detox	-0.63049	x 0.646	0.0207
NM_033597	myeloblastosis oncogene (Myb)	Transcript	-0.61924	x 0.65	0.0174
NM_021396	butyrophilin-like protein (Btdc)	Immun	-0.61661	x 0.652	0.0013
NM_008182	glutathione S-transferase, alpha 2 (Yc2) (Gsta2)	Enz, Detox	-0.61598	x 0.652	0.0069
NM_009405	troponin I, skeletal, fast 2 (Tnni2)	MCm	-0.61569	x 0.653	0.0417
NM_011704	vanin 1 (Vnn1)	Detox	-0.60899	x 0.656	0.0001
NM_009676	aldehyde oxidase 1 (Aox1)	Enz,	-0.60447	x 0.658	0.0047
NM_023785	pro-platelet basic protein (Ppbb)	Signal, Immun	-0.59965	x 0.66	0.0094
NM_018778	claudin 8	Epm	-0.59480	x 0.662	0.0003
NM_009994	cytochrome P450, 1b1, benz(a)anthracene inducible (Cyp1b1)	Enz, Detox	-0.59413	x 0.662	0.0115
NM_008165	glutamate receptor, ionotropic, AMPA1 (alpha 1) (Gria1)	Recept	-0.59078	x 0.664	0.0020
NM_008592	forkhead box C1 (Foxc1)	Transcript	-0.59037	x 0.664	0.0382
NM_007710	creatine kinase, muscle (Ckmm)	Enz, MCm	-0.58630	x 0.666	0.0162
NM_007617	caveolin 3	Signal, MCm	-0.58227	x 0.668	0.0273
NM_007933	enolase 3, beta muscle (Eno3)	Enz, MCm	-0.57902	x 0.669	0.0328
NM_009998	cytochrome P450, 2b10, phenobarbital inducible, type b (Cyp2b10)	Enz, Detox	-0.57377	x 0.672	0.0312
NM_008469	keratin complex 1, acidic, gene 15 (Krt1-15)	Epm	-0.56978	x 0.674	0.0318
NM_008419	potassium voltage-gated channel, member 5 (Kcna5)	Transport	-0.56587	x 0.676	0.0363
NM_007817	cytochrome p450, 2f2 (Cyp2f2)	Enz, Detox	-0.56285	x 0.677	0.0185
NM_013494	Carboxypeptidase E	Enz Prot metab	-0.56262	x 0.677	0.0022
NM_013712	integrin beta 1 binding protein 2	Recept, ECM	-0.56174	x 0.677	0.0013
NM_009814	calsequestrin 2 (Casq2)	MCm	-0.55415	x 0.681	0.0379
BQ174827	doublecortin and calcium/calmodulin-dependent protein kinase-like 1	Enz, Prot metab	-0.55458	x 0.68	0.0137
NM_007429	angiotensin II receptor, type 2 (Agtr2)	Recept	-0.55246	x 0.682	0.0302
NM_011098	Brx1a mRNA for homeoprotein	Transcript, MCm	-0.54870	x 0.684	0.0102
AF356844	carboxypeptidase Z	Enz, Prot metab	-0.54419	x 0.685	0.0292
NM_007751	cytochrome c oxidase, subunit VIIIb (Cox8b)	Enz, Detox	-0.53763	x 0.689	0.0133
NM_011782	a disintegrin-like and metalloprotease 5 (aggrecanase-2) (Adamts5)	Enz, ECM	-0.53751	x 0.689	0.0316
NM_023478	uroplakin 3 (Upk3)	Epm	-0.53425	x 0.69	0.0132
NM_008664	myomesin 2	MCm	-0.53029	x 0.692	0.0172
NM_009610	actin, gamma 2, smooth muscle, enteric (Actg2)	MCm	-0.52433	x 0.695	0.0404
NM_007868	dystrophin, muscular dystrophy (Dmd)	MCm	-0.52267	x 0.696	0.0067
NM_080462	histamine N-methyltransferase (Hmmt)	Enz, Immun	-0.52095	x 0.697	0.0221
NM_023617	aldehyde oxidase 3 (Aox3)	Retino metab	-0.51687	x 0.699	0.0094

NM_025711	asporin (Aspn)	ECM	-0.51470	x 0,7	0.0146
NM_007755	cytoplasmic polyadenylation element binding protein (Cpeb)	Prot metab	-0.51347	x 0,7	0.0004
NM_017370	haptoglobin (Hp)	Prot metab	-0.51060	x 0,702	0.0175
NM_008862	protein kinase inhibitor, alpha (Pkia)	Prot metab	-0.50431	x 0,705	0.0400
NM_016762	matrilin 2	ECM	-0.50199	x 0,706	0.0341
NM_010390	major histocompatibility complex Q1b	Immun	-0.50045	x 0,707	0.0203
NM_008242	forkhead box D1 (Foxd1)	Transcript	-0.50023	x 0,707	0.0268
NM_008785	serine (or cysteine) proteinase inhibitor, Clade A, member 5 (Serpina5)	Prot metab	-0.49974	x 0,707	0.0366
NM_009154	semaphorin 5A (Sema5a)	Migr	-0.49740	x 0,708	0.0409
NM_020621	pyrimidinergic receptor P2Y, G-protein coupled, 4 (P2ry4)	Recept	-0.49545	x 0,709	0.0116
M12233	actin, alpha 1, skeletal muscle (Acta1)	MCm	-0.49534	x 0,709	0.0005
NM_008522.1	lactotransferrin (Ltf)	Immun	-0.49078	x 0,712	0.0160
NM_053253.1	Blu protein (Blu)	Immun	-0.48146	x 0,716	0.0231
NM_009144.1	secreted frizzled-related sequence protein 2 (Sfrp2)	Prolif, EMT	-0.47671	x 0,719	0.0211
NM_011347.1	selectin, platelet (Selp)	Recept, Adh	-0.47634	x 0,719	0.0034
NM_019662.1	Ras-related associated with diabetes (Rrad)	Enz, GTPase	-0.47134	x 0,721	0.0293
NM_013669.1	synaptosomal-associated protein, 91 kDa (Snap91)	Synapse marker	-0.46817	x 0,723	0.0235
NM_024406.1	fatty acid binding protein 4, adipocyte (Fabp4)	Lipog	-0.46752	x 0,723	0.0406
AF357883.1	homeodomain transcription factor (Nkx6-1)	Transcript	-0.46167	x 0,726	0.0169
AF020738.1	fibroblast growth factor-related protein FGF-12A (Fgfl2)	Sign	-0.45776	x 0,728	0.0439
NM_022881.1	regulator of G-protein signaling 18 (Rgs18)	Signaling Regul	-0.45263	x 0,731	0.0325
NM_021467.2	troponin I, skeletal, slow 1 (Tnni1)	MCm	-0.44982	x 0,732	0.0163
NM_019417.1	PDZ and LIM domain 4 (Pdlim4)	Prot metab	-0.44649	x 0,734	0.0225
NM_010769.1	matrilin 1, cartilage matrix protein 1 (Matn1)	ECM	-0.44476	x 0,735	0.0280
NM_019738.1	nuclear protein 1 (Nupr1)	Transcript	-0.44316	x 0,736	0.0051
NM_023113.1	aspartoacylase (aminoacylase) 2	Enz, Prot metab	-0.43938	x 0,737	0.0050
NM_010669.1	keratin complex 2, basic, gene 6b (Krt2-6b),	Epm	-0.43792	x 0,738	0.0065
NM_130895.1	adenosine deaminase, RNA-specific, B1 (Adarb1)	Enz	-0.42746	x 0,744	0.0152
NM_031160.1	ADP-ribosylation factor 4-like (Arf4l)	Signaling Regul	-0.42584	x 0,744	0.0229
NM_011582.1	thrombospondin 4 (Thbs4)	ECM	-0.42420	x 0,745	0.0242
AF071068.1	aromatic-L-amino-acid decarboxylase	Enz	-0.42030	x 0,747	0.0194
NM_010016.1	decay accelerating factor 1 (Daf1)	Immun	-0.41955	x 0,748	0.0062
NM_011459.1	serine protease inhibitor 8 (Spi8)	Enz	-0.41851	x 0,748	0.0025
NM_007940.1	epoxide hydrolase 2, cytoplasmic (Ephx2)	Enz, Detox	-0.41824	x 0,748	0.0242
NM_007689.1	chondroadherin (Chad)	ECM	-0.41822	x 0,749	0.0327

772
773
774
775
776
777
778
779
780

Abbreviations: Funct. Cat., functional category of gene product; Adh, adhesion molecule; Detox, detoxification and xenobiotic metabolism; ECM, extracellular-matrix component or metabolism; Epm, epithelial marker; Enz, enzyme or enzyme inhibitor; Glycoconj, glycoconjugate metabolism; Immun, immune system; Inter metab, intermediary metabolism; Lipog, lipogenesis; MCm, muscle cell marker, Migr, cell migration; Prot metab, protein metabolism; Recept, receptor; Regul, regulator; Retino metab, retinoid metabolism, Signal, signaling molecule; Transcript, transcription factor or regulator; Transport, transporter molecule.

Genes with name and symbol in bold character had changes checked by RT-qPCR.

781

782 Table 6. Comparison of RT-qPCR data normalization by 18S rRNA and Hprt1 mRNA. Developmental
 783 changes of expression levels in the lung of 4 genes of interest (2 up-regulated and 2 down-regulated
 784 genes given as examples) are presented (arbitrary unit of $2^{-\Delta\Delta Ct}$ related to the expression of a
 785 calibrator sample).

786

	Adrenomedullin		Bone sialoprotein		C1qtnf3		Crabp1	
Reference gene	18S	Hprt1	18S	Hprt1	18S	Hprt1	18S	Hprt1
Day 0	0.51±0.11	0.72±0.13	0.25±0.07	0.40±0.15	0.61±0.18	1.10±0.50	0.02±0.00	0.03±0.01
Day 4	0.13±0.03*	0.20±0.01*	1.22±0.09*	2.33±0.67*	1.99±0.42*	3.42±0.46*	0.08±0.02*	0.14±0.03*
Day 7	0.50±0.16*	0.59±0.02*	1.04±0.26	1.33±0.19*	1.10±0.11*	1.55±0.21*	0.46±0.03*	0.67±0.12*
Day 10	0.75±0.30	1.10±0.26	0.66±0.22*	1.07±0.29	0.85±0.16	1.72±0.46	0.71±0.16*	1.27±0.15*
Day 14	0.49±0.13	1.52±0.17	0.04±0.01*	0.13±0.01*	0.35±0.06*	1.34±0.15	0.83±0.10	3.19±0.26*
Day 20	0.21±0.04*	0.76±0.11*	0.01±0.00*	0.04±0.01*	0.22±0.08	0.77±0.09*	0.33±0.09*	1.27±0.06*
Day 28	0.17±0.04	0.51±0.17	0.01±0.00	0.02±0.01	0.25±0.09	0.69±0.17	0.09±0.01*	0.29±0.05*
Adult	0.06±0.02*	0.36±0.05	0.01±0.00	0.02±0.01	0.05±0.02*	0.34±0.06*	0.01±0.00*	0.03±0.02*

787

788 Mean ± se on 4 individual determinations per stage.*Significant difference from preceding stage ($P < 0.05$ by U test).

789 Gene symbols: C1qtnf3 = C1q and tumor necrosis factor related protein 3; Crabp1: cellular retinoic acid binding protein 1.

790 Table 7. RT-qPCR determination of expression levels of 11 selected genes found to be up regulated by
 791 FGF18- transgene induction in microarray experiment.
 792

Genes	transcript level ($2^{\Delta\Delta Ct}$)		% of mean control level per litter	
	control pups	double-transgenic pups	control pups	double-transgenic pups
<i>Angiogenesis</i>				
Adrenomedullin	2.16 ± 0.26	14.23 ± 2.59***	100.0 ± 9.6	686.1 ± 136.1***
Wnt2	2.47 ± 0.32	5.54 ± 0.74***	100.0 ± 7.5	242.5 ± 39.4**
<i>ECM components</i>				
Bone sialoprotein	1.95 ± 0.20	4.99 ± 0.70***	100.0 ± 7.7	281.4 ± 61.6**
Fibulin 1	1.83 ± 0.23	2.91 ± 0.23*	100.0 ± 6.9	168.6 ± 14.7**
<i>Cell migration</i>				
Snai1	2.54 ± 0.38	3.97 ± 0.42*	100.0 ± 8.1	161.4 ± 16.2**
Snai2	2.42 ± 0.31	5.51 ± 1.21*	100.0 ± 8.1	242.4 ± 59.8*
Ptger2	1.31 ± 0.12	2.31 ± 0.26**	100.0 ± 7.0	176.5 ± 20.7**
<i>Antioxidant mech.</i>				
Gstm5	1.69 ± 0.21	5.09 ± 0.86***	100.0 ± 7.7	321.43 ± 64.2**
Ceruloplasmin	1.96 ± 0.38	4.54 ± 0.66**	100.0 ± 12.3	263.17 ± 52.7**
<i>Other</i>				
CD36 antigen	2.37 ± 0.42	4.97 ± 0.74**	100.0 ± 10.7	250.8 ± 38.0**
Hsd11b1	1.33 ± 0.14	6.10 ± 1.17***	100.0 ± 8.5	491.0 ± 102.1***

793

794 Mean ± se on 10 control pups and 11 double-transgenic pups from 5 different litters. Difference with control group (one-
 795 tailed t test for unpaired data) for: * $P < 0.05$; ** $P < 0.01$; *** $P < 0.001$. Genes are presented in decreasing order of stimulation
 796 gained from microarray analysis. Gene symbols: Hsd11b1 = hydroxysteroid 11-beta dehydrogenase 1; Gstm5 = glutathione
 797 S-transferase, mu5; Wnt2 = wingless-related MMTV integration site 2; Snai = snail homolog; PgEPR EP2 = prostaglandin E
 798 receptor, EP2 subtype.

799

800

801

802

803 Table 8. RT-qPCR determination of expression levels of 10 selected genes found to be down regulated
 804 by FGF18-transgene induction in microarray experiment.
 805

Genes	transcript level ($2^{\Delta\Delta C_t}$)		% of mean control level per litter	
	control pups	double-transgenic pups	control pups	double-transgenic pups
<i>Adipocyte and/or alveolar typeII-cell markers</i>				
C1qtnf3	1.10 ± 0.16	0.62 ± 0.19*	100.0 ± 8.6	50.9 ± 12.7**
Stearoyl-CoA desaturase 1	1.83 ± 0.24	0.57 ± 0.06***	100.0 ± 9.7	30.7 ± 3.4***
Abca3	1.52 ± 0.49	0.84 ± 0.32***	100.0 ± 20.9	54.8 ± 15.6***
<i>Other epithelial-cell markers</i>				
Cyp1b1	1.31 ± 0.18	0.96 ± 0.12*	100.0 ± 7.6	76.1 ± 9.6*
Sox2	1.24 ± 0.20	1.29 ± 0.14 ^{ns}	100.0 ± 7.9	93.4 ± 13.7 ^{ns}
<i>ECM and ECM metabolism</i>				
Osteoglycin	1.92 ± 0.33	1.70 ± 0.43 ^{ns}	100.0 ± 10.8	94.2 ± 24.1 ^{ns}
Fap/seprase	1.60 ± 0.90	1.51 ± 0.99 ^{ns}	100.0 ± 8.1	104.4 ± 28.0 ^{ns}
<i>Cell migration/invasion</i>				
Doublecortin	1.80 ± 0.20	1.13 ± 0.28*	100.00 ± 9.89	63.0 ± 16.9*
<i>Retinoic acid metabolism</i>				
Crabp1	1.74 ± 0.17	0.72 ± 0.26**	100.0 ± 7.5	41.4 ± 19.9**
Aldh1a1	1.83 ± 0.18	2.29 ± 0.45 ^{ns}	100.0 ± 8.1	133.1 ± 27.9 ^{ns}

806

807 Mean ± se on 10 control pups and 11 double-transgenic pups from 5 different litters. Difference with control group (one-
 808 tailed t test for unpaired data) for: * $P < 0.05$; ** $P < 0.01$; *** $P < 0.001$; ns = not significant. Genes are presented in decreasing
 809 order of inhibition gained from microarray analysis. Gene symbols and abbreviation: C1qtnf3 = C1q and tumor necrosis
 810 factor related protein 3; CoA = coenzyme A; Abca3 = ATP-binding cassette transporter ABCA3; Fap = fibroblast activation
 811 protein; Crabp1: cellular retinoic acid binding protein 1; Sox2 = SRY-box containing gene 2; Aldh1a1 = aldehyde
 812 dehydrogenase 1, subfamily A1; Cyp1b1 = cytochrome P450, 1b1.

813

814

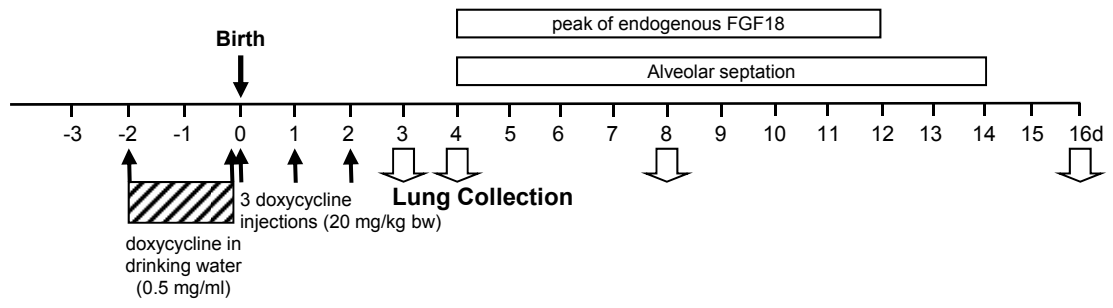


Figure 1

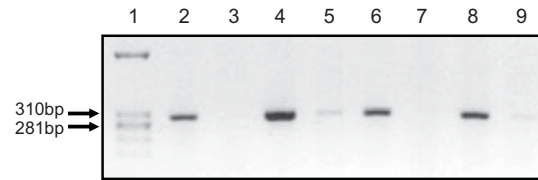


Figure 2

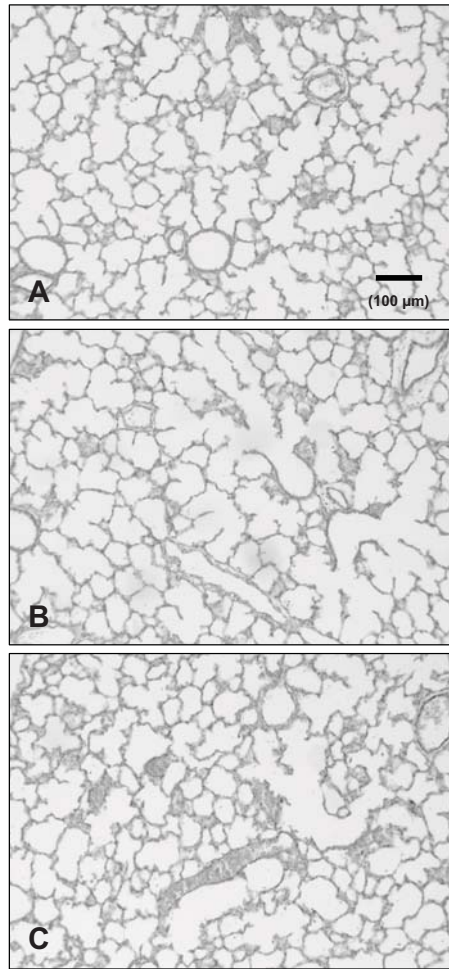


Figure 3

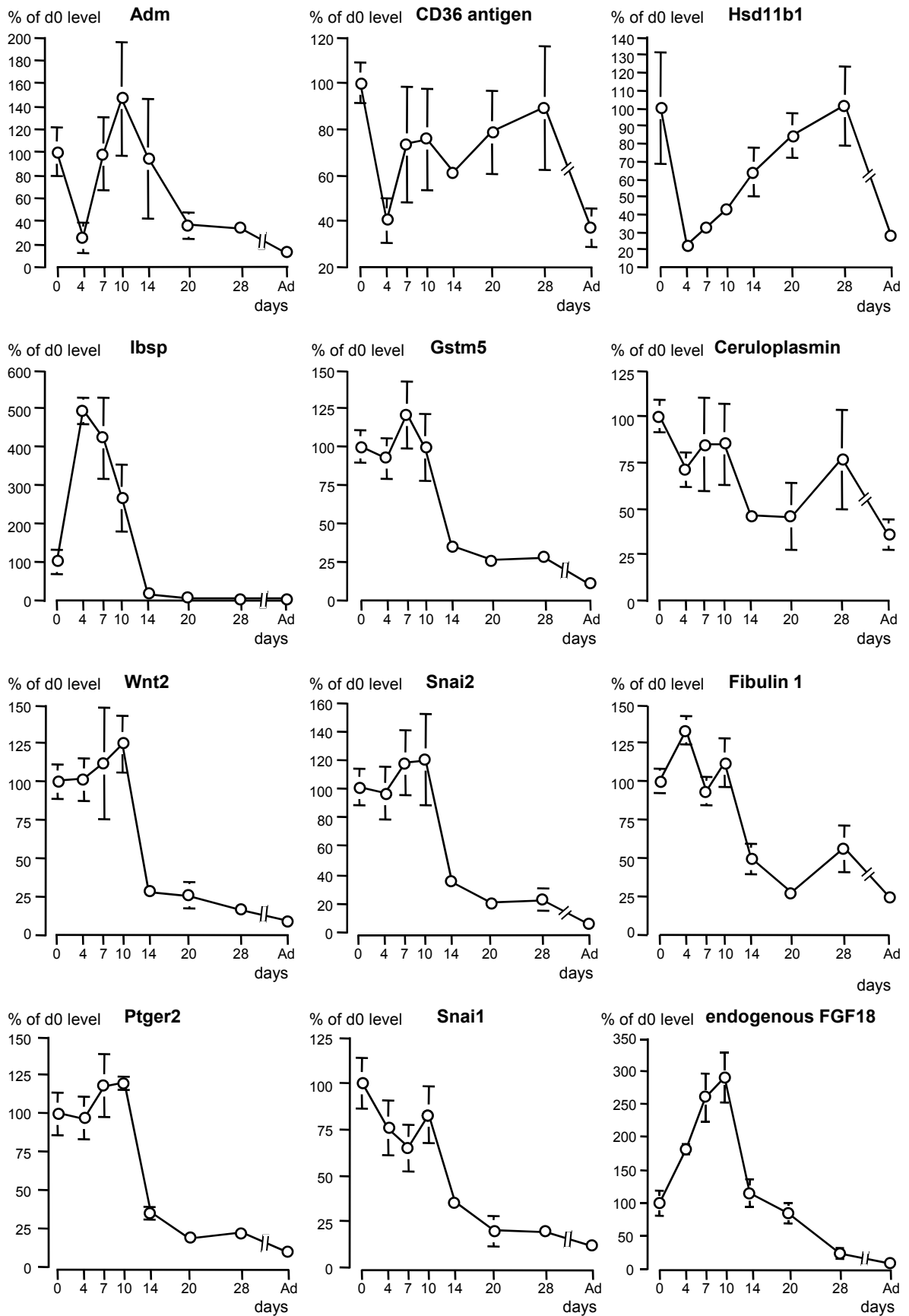


Figure 4

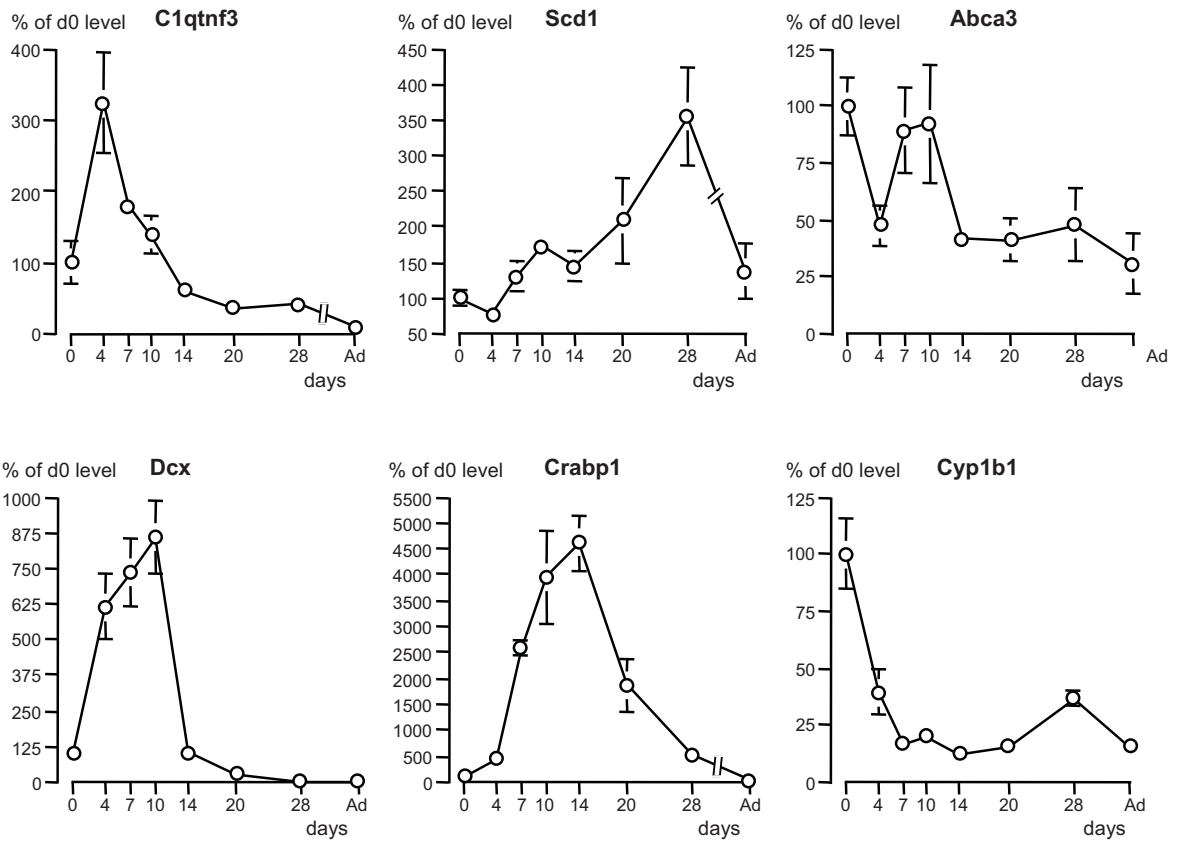


Figure 5